Evoked otoacoustic emissions arise by two fundamentally different mechanisms: A taxonomy for mammalian OAEs

Christopher A. Shera[a] and John J. Guinan, Jr.
Eaton-Peabody Laboratory of Auditory Physiology, Massachusetts Eye and Ear Infirmary, 243 Charles Street, Boston, Massachusetts 02114 and Department of Otology and Laryngology, Harvard Medical School, Boston, Massachusetts 02115

(Received 2 June 1998; accepted for publication 27 October 1998)

Otoacoustic emissions (OAEs) of all types are widely assumed to arise by a common mechanism: nonlinear electromechanical distortion within the cochlea. In this view, both stimulus-frequency (SFOAEs) and distortion-product emissions (DPOAEs) arise because nonlinearities in the mechanics act as ''sources'' of backward-traveling waves. This unified picture is tested by analyzing measurements of emission phase using a simple phenomenological description of the nonlinear re-emission process. The analysis framework is independent of the detailed form of the emission sources and the nonlinearities that produce them. The analysis demonstrates that the common assumption that SFOAEs originate by nonlinear distortion requires that SFOAE phase be essentially independent of frequency, in striking contradiction with experiment. This contradiction implies that evoked otoacoustic emissions arise by two fundamentally different mechanisms within the cochlea. These two mechanisms (linear reflection versus nonlinear distortion) are described and two broad classes of emissions—reflection-source and distortion-source emissions—are distinguished based on the mechanisms of their generation. The implications of this OAE taxonomy for the measurement, interpretation, and clinical use of otoacoustic emissions as noninvasive probes of cochlear function are discussed. © *1999 Acoustical Society of America.* [S0001-4966(99)02202-X]

PACS numbers: 43.64.Jb, 43.64.Kc, 43.64.Bt [BLM]

INTRODUCTION

During the 20 years since Kemp's (1978) discovery, otoacoustic emissions (OAEs) have become widely used, both as research tools and as clinical diagnostic and screening aids (e.g., Kemp *et al.*, 1986; Norton and Stover, 1994; Whitehead *et al.*, 1996a; Robinette and Glattke, 1997). Interpretation of measured otoacoustic responses is grounded on an underlying picture of the origin of evoked OAEs. All categories of evoked OAEs are commonly regarded as originating in nonlinear distortion, presumably through the electromotile responses of outer hair cells (Brownell, 1990). These nonlinearities in cochlear mechanics are thought to act as ''sources'' of backward-traveling waves (Kemp, 1978; de Boer, 1983; Allen and Neely, 1992). Kemp (1997) describes the physical mechanism—often simply abstracted as ''nonlinear stimulus re-emission'' by cellular ''emission generators''—in a recent review:

> ''The model of the phenomenon adopted at that time [circa 1978] is still relevant. It is that ... a nonlinearity at the peak of the traveling wave turns around or scatters back some of the traveling wave energy, and returns both stimulus frequency and intermodulation signals back to the middle ear.''

We epitomize in Table I the major elements of this ''common view''—and the nonlinear-distortion model that underlies it—as culled from the literature (e.g., Kemp, 1980, 1998; Probst *et al.*, 1991; Allen and Neely, 1992; Allen and Lonsbury-Martin, 1993; Patuzzi, 1996; Hartmann, 1997).[1]

In this paper, *we argue that the common view cannot be correct*. For although the nonlinear-distortion model accounts for distortion products, it cannot explain stimulus-frequency or transiently evoked emissions, in particular their phase, which rotates rapidly with frequency at low sound levels. Although considerably elaborated, our central argument is similar in spirit to that first used by Kemp and Brown (1983a) and later formalized by others (Strube, 1989; Shera and Zweig, 1993b; Zweig and Shera, 1995) to distinguish ''wave-'' and ''place-fixed'' emission mechanisms. By combining our argument with data on emission phase, we conclude that at low sound levels stimulus-frequency and transiently evoked emissions must arise by mechanisms fundamentally different from pure distortion products.[2] We therefore distinguish two classes of emissions—reflection- and distortion-source emissions—based on the mechanisms of their generation. Our mechanism-based taxonomy has important implications for the measurement, interpretation, and use of otoacoustic emissions as noninvasive probes of cochlear function.[3]

I. DEFINITIONS AND BACKGROUND

Otoacoustic emissions are typically classified according to the stimulus waveform and related details of the measurement paradigm (e.g., Zurek, 1985). Initially, we follow suit by distinguishing two classes of evoked emissions based on the relationship between the emissions and the stimuli used to elicit them:[4]

[a]Electronic mail: shera@epl.meei.harvard.edu

TABLE I. Synopsis of the ''common view'' of evoked emissions presented in the literature.

Common view of evoked emissions
• Evoked otoacoustic emissions arise through nonlinear stimulus ''re-emission'' by cellular ''emission generators'' (e.g., outer hair cells). • Stimulus re-emission occurs because electromechanical nonlinearities—principally those near the peak of the traveling-wave envelope—act as ''sources'' of backward-traveling waves. • SFOAEs and DPOAEs both arise through nonlinear distortion (e.g., SFOAEs can be thought of as ''zeroth-order'' DPOAEs arising from distortion at the first harmonic).

(i) Echo emissions comprise stimulus-frequency and transiently evoked emissions (SFOAEs and TEOAEs), grouped together because they occur at the frequency (or frequencies) of stimulation, whether the stimulus is a pure tone or an acoustic transient.

(ii) Distortion-product emissions (DPOAEs) occur at frequencies not present in the evoking stimulus (e.g., at the frequency $2f_1-f_2$ in response to stimulus tones at frequencies f_1 and f_2).

Our use of the distortion-product nomenclature is standard, and we introduce the term ''echo emissions'' simply as a convenient shorthand. In the common view these two classes of evoked emission both arise from nonlinear electromechanical distortion within the cochlea. Preparatory to further analysis, we review basic properties of echo emissions at low sound levels.

A. Characterizing echo emissions at low levels

As one sweeps the frequency of an acoustic stimulus tone, the pressure in the human ear canal, P_{ec}, varies as shown in Fig. 1. As the stimulus level is lowered, a regular oscillatory component appears superposed on a more smoothly varying ''background'' response. Whereas the shape of the background depends on the acoustics of the ear canal and middle ear, the oscillatory component represents an acoustic interference pattern created by the superposition of the stimulus tone and a second tone at the same frequency originating from within the cochlea (Kemp, 1978, 1979a,b). The relative amplitude of the oscillatory component grows as the stimulus level is reduced, until, at the sound levels near threshold shown in Fig. 2 ($\lesssim$5 dB SL), the interference pattern becomes approximately independent of sound level, indicating that stimulus and response are linearly related (Zwicker and Schloth, 1984; Shera and Zweig, 1993a). Similar quasi-periodic oscillations appear in the frequency spectra of the responses to low-level acoustic transients (e.g., Zwicker and Schloth, 1984).[5] At frequencies near 1500 Hz, the frequency spacing Δf_{OAE} between adjacent spectral maxima is approximately 100 Hz in human ears.

1. Interpretation using the cochlear traveling-wave reflectance, R

We interpret evoked emissions as indicating the presence of backward-traveling waves within the cochlea. To characterize their properties, we define the *cochlear traveling-wave reflectance*, *R*, as the complex ratio of the out-going (or emitted) pressure wave to the in-going (or stimulus) wave at the basal end of the cochlea near the stapes (Shera and Zweig, 1993a):[6]

$$R(f;A)\equiv\left.\frac{P_{\text{out-going}}}{P_{\text{in-going}}}\right|_{\text{stapes}}, \tag{1}$$

where *R* depends on both the frequency, *f*, and amplitude, *A*, of the stimulus. The cochlear reflectance provides a phenomenological characterization of the emission process as seen from the base of the cochlea.[7]

By regarding the intervening middle ear as a linear, two-port network, one can relate the cochlear reflectance, *R*, to measurements of ear-canal pressure, P_{ec} (Shera and Zweig, 1993a). When the emission amplitude is small relative to the stimulus ($|R|\ll 1$), the relation reduces to the simple formula[8]

$$\frac{P_{ec}(f;A)}{P_{ec}(f;A_{ref})}\approx\frac{A}{A_{ref}}[1+m(f)R(f;A)], \tag{2}$$

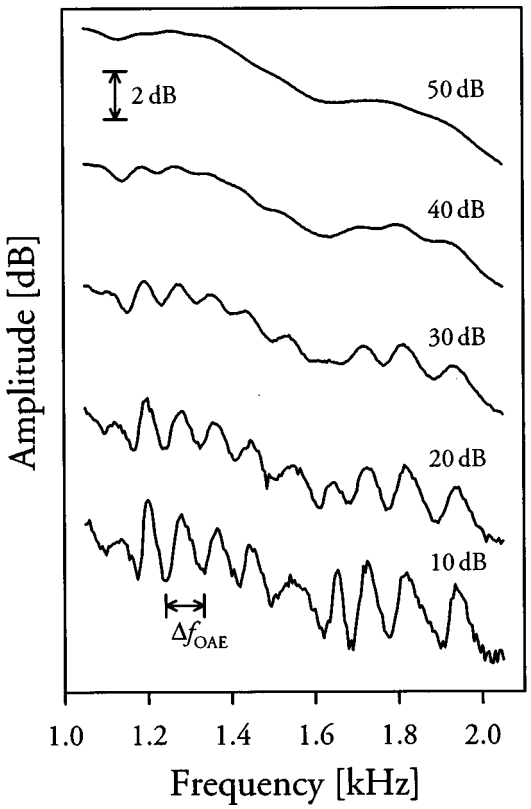

FIG. 1. Frequency dependence of ear-canal pressure and its variation with sound level in a normal human ear. The curves, offset vertically from one another for clarity, represent the normalized amplitude of the ear-canal pressure, P_{ec}, measured with a constant voltage applied to the earphone driver (Shera and Zweig, 1993a). The approximate sensation level of the stimulus tone at 1300 Hz is indicated on the right. At the highest level the pressure amplitude varies relatively smoothly with frequency. As the stimulus level is lowered, sound generated within the cochlea combines with the stimulus tone to create an oscillatory acoustic interference pattern that appears superposed on the smoothly varying background seen at high levels. Near 1500 Hz, the frequency spacing Δf_{OAE} between adjacent spectral maxima is approximately 100 Hz. Data from Shera and Zweig (1993a).

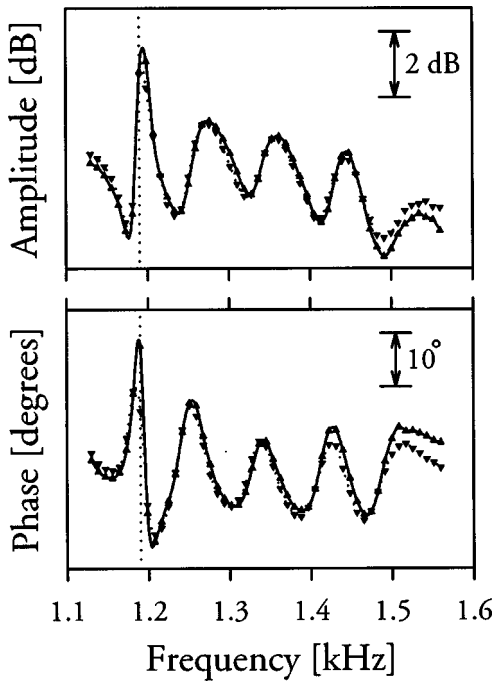

FIG. 2. Linearity at low levels manifest by measurements of the ear-canal pressure, P_{ec}, normalized by the amplitude of the earphone-driver voltage, at sound levels of 5 dB SL (▲) and 0 dB SL (▼) relative to threshold at 1300 Hz. The vertical dotted line marks the frequency of a known spontaneous emission. Aside from a small drift in the background—probably the result of slow changes in middle-ear cavity pressure and/or variations in the temperature of the recording microphone—the two functions nearly superpose, indicating that the response appears linear at these near-threshold levels. Adapted from Fig. 6 of Shera and Zweig (1993a).

where A is the stimulus amplitude and A_{ref} is a high-level reference amplitude at which the relative amplitude of the emissions is negligible (e.g., in humans $A_{ref} \approx 60$ dB SPL). The complex function $m(f)$ characterizes round-trip middle-ear transmission and varies relatively slowly with frequency (Shera and Zweig, 1993a).

At sound levels near threshold, R becomes independent of level, indicating that the emitted wave varies linearly with the stimulus. Solving Eq. (2) for mR using measurements of P_{ec} yields a function of slowly varying amplitude and rapidly rotating phase (Shera and Zweig, 1993a). Typical results, obtained from the measurements of Fig. 2 in the low-level linear regime, are shown in Fig. 3. Although the function $m(f)$ characterizing middle-ear transmission is not known in detail, middle-ear transfer functions vary relatively slowly with frequency compared to the oscillations in the ear-canal pressure spectrum (e.g., Puria *et al.*, 1997; Puria and Rosowski, 1997). The frequency dependence of the product mR is therefore primarily that of the reflectance R. Reference to Fig. 3 shows that[9]

$$\text{Emission measurements} \Rightarrow \begin{cases} |R| \approx \text{slowly varying} \\ \angle R \approx \text{locally linear with } f. \end{cases} \tag{3}$$

Over frequency intervals corresponding to a few oscillations in the pressure spectrum (i.e., over intervals a few times the size of Δf_{OAE}), the reflectance R has the approximate form[10]

$$R(f) \approx |R| e^{-2\pi i f \tau}, \tag{4}$$

where the amplitude $|R| \approx$ constant and $\tau \approx 10$ ms near 1500 Hz. Whereas the amplitude of the reflectance varies slowly, its phase rotates rapidly, circling one full period over the frequency interval $\Delta f_{OAE} \approx 1/\tau$. Since the largest contributions to the emission are believed to originate near the peak of the forward-traveling wave, the approximate constancy of $|R|$ suggests—via the cochlear mapping between frequency and position—that all points along the cochlear partition are about equally effective at reflecting the traveling wave. The linear variation of $\angle R$ with frequency suggests the presence of a delay (in this case, of about 10 ms).

Although deduced from measurements of stimulus-frequency emissions, Eq. (4) can be reinterpreted in the time domain to provide a description of transiently evoked emissions valid in the low-level linear regime: The echo evoked by a narrow-band tone burst is a scaled (by a factor $|R|$) and delayed (by τ seconds) version of the stimulus waveform (e.g., Wilson, 1980; Norton and Neely, 1987).[11] Having characterized the properties of echo emissions at low levels, we next consider whether they can originate through nonlinear distortion.

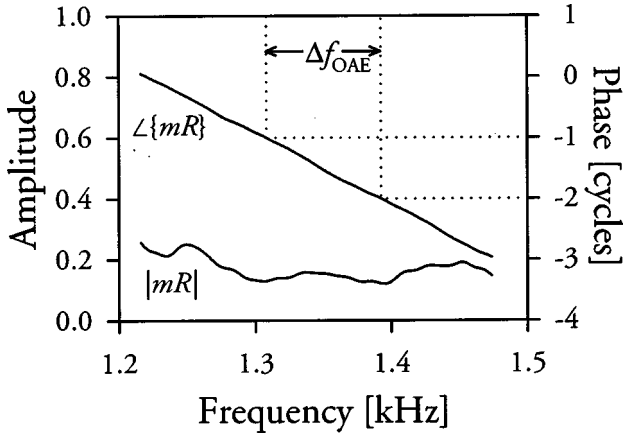

FIG. 3. Amplitude and phase of mR versus frequency computed from a subset of the data in Fig. 2 that avoids the spontaneous emission (Shera and Zweig, 1993a). The curves indicate that R has a slowly varying amplitude and a locally linear phase (assuming m is slowly varying). The frequency interval Δf_{OAE} between spectral maxima in ear-canal pressure corresponds to a full rotation of the phase of R. Data from Shera and Zweig (1993a).

II. DO ECHO EMISSIONS ARISE BY NONLINEAR DISTORTION?

A. The nonlinear-distortion model

The nonlinear-distortion model that underlies the common view of evoked emissions is illustrated schematically in Fig. 4. When the cochlear response is nonlinear, traveling waves can induce spatial distortions in the mechanics that act as ''sources'' of backward-traveling waves. In addition to accounting for distortion-product emissions, the model also appears to provide a natural explanation for echo emissions. For example, the observation that $|R| \approx$slowly varying—that is, that all points ''reflect'' about equally—might be naturally explained by supposing that the sources that generate the backward-traveling wave are induced by the wave itself through nonlinearities in the mechanics (Kemp, 1978, 1979a;

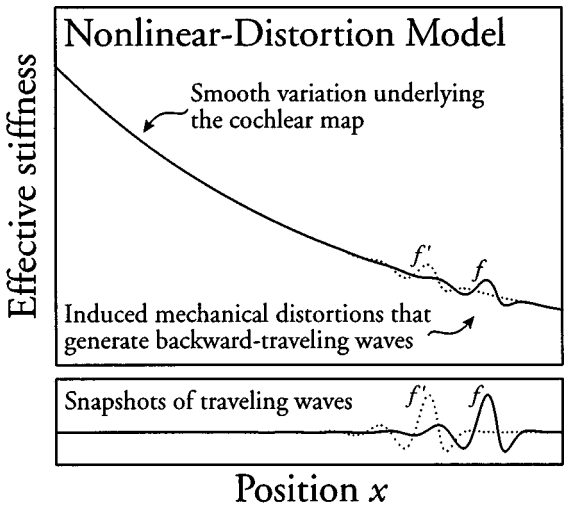

FIG. 4. Mechanical distortions induced by pure-tone stimulation. When the cochlear response is nonlinear, the traveling wave (bottom panel) is presumed to induce distortions in the mechanics (top panel) that act as sources of backward-traveling waves. In the example shown here, the traveling wave induces distortions in the effective stiffness of the cochlear partition (e.g., via nonlinearities in the mechanisms of force generation by outer hair cells). The dotted line shows how the region of induced mechanical distortion moves with the wave envelope as the stimulus frequency is increased from f to f'.

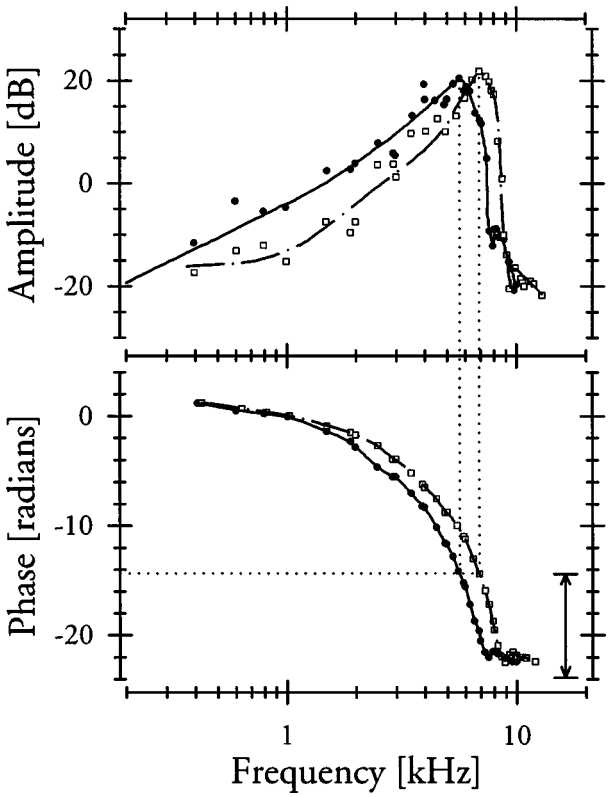

FIG. 5. Constancy of phase accumulation at the peak of the wave envelope. The figure shows Rhode's (1971, Fig. 8) measurements of basilar-membrane transfer functions (i.e., basilar membrane to malleus displacement ratios) at two nearby positons along the basilar membrane ($\Delta x \approx 1.5$ mm). As indicated by the dotted lines, the total phase accumulation at the peak of the transfer function (horizontal line) is not a strong function of frequency (vertical lines). The scale bar (double-headed arrow) in the lower right-hand corner provides an estimate of the relative phase accumulation necessary to account for the rapid rotation of $\angle R$ (see footnote 12). Relative to the scale bar, the observed difference in phase accumulation is negligible.

de Boer, 1983; Allen and Neely, 1992). And, since the phase of R has the form of a delay, it is natural to associate that delay with wave travel to and from the site of generation of the re-emitted wave.

An attractive feature of the nonlinear-distortion model is its implicit unification of echo and distortion-product emissions through a common origin in cochlear nonlinearity. Intuitively, the model seems to account naturally for both striking features of the frequency dependence of R (i.e., $|R| \approx$slowly varying, since the induced sources depend on the form and strength of cochlear nonlinearities, which presumably vary relatively slowly with position; and $\angle R \approx$locally linear with frequency, due to the round-trip traveling-wave delay between the stapes and the site of re-emission).

In what follows, we analyze the model more carefully and show that *the nonlinear-distortion model*—despite its apparent virtues—*actually predicts a constant reflectance phase, in striking contradiction with experiment*.

B. Can the nonlinear-distortion model account for $\angle R$?

To simplify the analysis of the model without sacrificing any essential feature, we assume that the forward-traveling wave is re-emitted by a nonlinear source induced at the *peak* of the traveling wave. Recall that $\angle R$ represents the accumulated phase shift between the out- and in-going waves at the stapes. In our simplified nonlinear-distortion model, this phase shift can be written as the sum of three components:

$$\angle R = \Delta\theta_{\text{forward-travel}} + \Delta\theta_{\text{re-emission}} + \Delta\theta_{\text{reverse-travel}}, \qquad (5)$$

representing phase shifts due to forward and reverse wave propagation (i.e., between the stapes and the site of re-emission at the peak of the wave envelope) and any phase shift due to the re-emission process itself. Consistency with the data of Fig. 3 requires that the sum of these phase shifts rotate rapidly with frequency. Does the model agree with experiment?

1. Phase shifts due to wave travel cannot account for $\angle R$

First, we consider phase shifts due to wave travel. Does $\Delta\theta_{\text{forward}}$ rotate rapidly with frequency? Figure 5 answers this question using measurements of basilar-membrane motion. The figure shows the phase accumulated by the forward-traveling wave as it propagates from the stapes to the peak of its envelope at its characteristic place. Perhaps surprisingly, the phase accumulation at the peak of the wave envelope is almost independent of frequency:

$$\underset{\text{measurements}}{\text{Basilar-membrane}} \Rightarrow \Delta\theta_{\text{forward-travel}} \approx \text{constant}. \qquad (6)$$

For comparison, the scale bar in Fig. 5 illustrates the phase shift necessary to account for the estimated change in $\angle R$ over the same frequency range.[12] Relative to the scale bar, the observed difference in the phase accumulation is negligible.

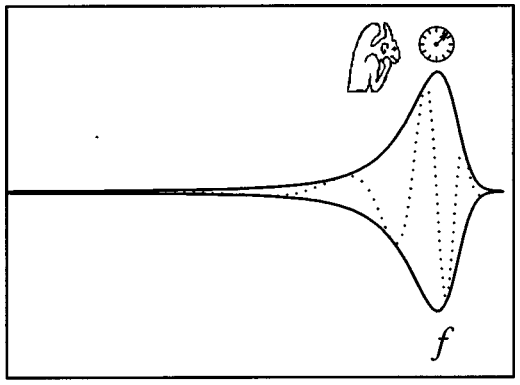

FIG. 6. The demon emitter. Charged with generating emissions by pushing and pulling on the basilar membrane, the demon needs to determine the stimulus frequency in order to create a backward-traveling wave with the correct relative phase. To determine the stimulus frequency the demon must compare the period of basilar-membrane vibration with the ticking of a ''clock.'' The only clock available, however, is the local resonator that determines the characteristic frequency.

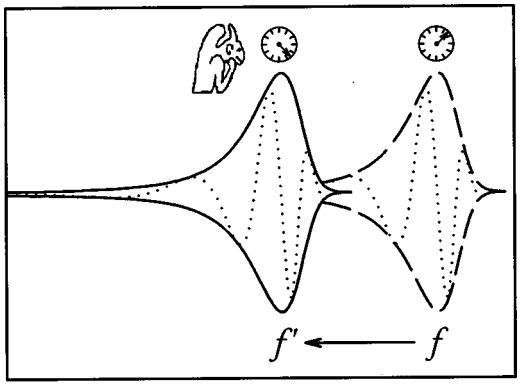

FIG. 7. When the stimulus frequency is changed (e.g., from $f \rightarrow f'$), the envelope of the traveling wave shifts along the basilar membrane. Because the demon moves with the wave, changing the stimulus frequency changes the demon's local time reference correspondingly. As a result, the demon cannot detect changes in stimulus frequency and thus cannot generate backward-traveling waves whose phase depends on that frequency.

The constancy of $\Delta\theta_{\text{forward}}$ is an immediate consequence of the approximate local scaling symmetry (Zweig, 1976; Siebert, 1968; Sondhi, 1978) manifest by basilar- and tectorial-membrane transfer functions (Rhode, 1971; Gummer *et al.*, 1987; Rhode and Cooper, 1996) and neural tuning curves (e.g., Kiang and Moxon, 1980; Liberman, 1978). Local scaling symmetry implies that rather than depending on position and frequency independently, basilar-membrane transfer functions depend on the two variables x and f only in the single combination $f/f_{\text{cf}}(x)$, where $f_{\text{cf}}(x)$ is the cochlear position-frequency map. When the cochlear map is exponential, the symmetry implies that traveling-wave envelopes are locally ''shift-similar,'' with the number of wavelengths in the traveling wave nearly independent of frequency. Compared to the higher frequency wave, the lower frequency wave travels further along the cochlea and requires a longer time to reach its peak. But *both waves travel the same number of wavelengths*, and the total phase accumulation is therefore the same.

Although we have no direct measurements of the phase shift $\Delta\theta_{\text{reverse}}$,[13] standard cochlear models[14] predict that

$$\Delta\theta_{\text{reverse-travel}} \approx \Delta\theta_{\text{forward-travel}}. \tag{7}$$

Consequently,[15]

$$\begin{matrix}\text{Measurements} \\ \text{and models}\end{matrix} \Rightarrow \Delta\theta_{\text{round-trip}} \approx \text{constant}. \tag{8}$$

For the nonlinear-distortion model of echo emissions to agree with experiment, the phase rotation of $\angle R$ must originate in $\Delta\theta_{\text{re-emission}}$. To test whether this is possible, we consider the thought-experiment of the demon emitter.

2. Phase shifts due to re-emission cannot account for $\angle R$

Rather than bog ourselves down in the model-dependent—and, for our purposes, irrelevant—details of a particular nonlinear re-emission mechanism, we argue more generally by imagining that emissions are generated within the cochlea by a tiny demon who ''surfs'' the peak of the envelope of the traveling wave, where the effects of nonlinear distortion are presumably greatest (see Fig. 6).[16] The demon, agent for nonlinear distortion, is charged with launching backward-traveling waves by pushing and pulling on the basilar membrane. In the process, the demon introduces the phase shift $\Delta\theta_{\text{re-emission}}$. Can the demon supply the frequency dependence necessary to produce the observed form of $\angle R$?

At first sight, the answer appears to be ''Yes.'' For example, when the ear is stimulated with a pure tone the demon simply determines the stimulus frequency and consults a formula he keeps in his pocket that tells him how to compute, as a function of frequency,[17] the phase with which he must push and pull (relative to the local motion of the basilar membrane) in order to produce the appropriate value of $\Delta\theta_{\text{re-emission}}$.[18]

How does the demon determine the stimulus frequency?[19] From his position atop the traveling-wave envelope the demon counts the number of times the basilar membrane rises and falls and compares that number with the ticking of a ''clock.'' But what clock does he have available? The demon's time reference is the local ''resonator'' that determines the characteristic frequency, f_{cf}, at his location.[20] The demon's clock therefore ticks at intervals proportional to $1/f_{\text{cf}}$,[21] counting out time in units appropriate to his position along the cochlear partition.

Suppose that we fix the stimulus frequency at some value, f. Because the demon sits at the peak of the traveling wave (i.e., at the characteristic place corresponding to frequency f), he sees the basilar membrane undergo one oscillation for every tick of his clock (since $f/f_{\text{cf}}=1$). The demon concludes that the stimulus has unit frequency (in units of cycles/clock-tick) and, after evaluating his formula, pushes and pulls on the basilar membrane appropriately. For example, at unit frequency the demon might push downwards on the basilar membrane during every upwards zero-crossing of its local motion.

Now suppose that we increase the stimulus frequency to the value f' as illustrated in Fig. 7. By increasing the fre-

quency, we shift the envelope of the traveling wave basalwards towards the stapes. And the demon, because he surfs the envelope, is carried along with the wave (just as the sources induced by nonlinear distortion move with the wave; cf. Fig. 4). Again the demon determines the stimulus frequency by counting the number of basilar-membrane oscillations per clock tick. But note that *because he moved with the wave, the demon now uses a different clock*. He now uses the local resonator corresponding to his new location, and that resonator ticks at time intervals of $1/f'_{\rm cf}$. Thus, once again, the demon measures a frequency of 1 cycle/clock-tick (since $f'/f'_{\rm cf}=1$) and, after consulting his formula, pushes and pulls with the same relative phase that he did for frequency f.

Although the stimulus frequency changes ($f\rightarrow f'$), the demon's clock changes correspondingly ($f_{\rm cf}\rightarrow f'_{\rm cf}$). As a result, the demon cannot detect the change and so pushes and pulls with the same relative phase at all stimulus frequencies. The demon—a proxy for nonlinear distortion, or, indeed, any emission mechanism that moves with the wave envelope—cannot generate backward-traveling waves with a phase shift that depends on frequency:[22]

$$\begin{matrix}\text{Thought}\\ \text{experiment}\end{matrix}\Rightarrow \Delta\theta_{\text{re-emission}}\approx \text{constant}. \tag{9}$$

As suggested by the appearance in the thought-experiment of the relative frequency $f/f_{\rm cf}(x)$, this conclusion can be understood, equivalently, as a consequence of local scaling symmetry (Shera and Zweig, 1993b; Zweig and Shera, 1995).

By combining the predicted phase shifts due to wave travel and reflection we conclude that *the nonlinear-distortion model predicts a constant reflectance phase, in striking contradiction with experiment*:

$$\begin{matrix}\text{Nonlinear}\\ \text{distortion model}\end{matrix}\Rightarrow \angle R\approx \text{constant}. \tag{10}$$

Although the measured $\angle R$ varies rapidly with frequency, the nonlinear-distortion model predicts a constant value for each of the three component phase shifts in Eq. (5). *This contradiction effectively rules out nonlinear distortion as the origin of echo emissions at low levels.*

Note that our analysis of the nonlinear-distortion model is independent of the detailed form of the emission sources and the nonlinearities that produce them. Made above for simplicity, the assumption that emissions originate from a single point (e.g., from the peak of the wave envelope) is not critical to the conclusion. The argument is easily generalized—by considering many demons surfing many different parts of the wave—to include emissions created over a broad region of the cochlea.

C. Testing the predictions of the thought-experiment using DPOAEs

Our analysis of the nonlinear-distortion model can be tested experimentally by measuring the frequency dependence of emission phase under circumstances where the generation mechanism is *known* to be scaling-symmetric nonlinear distortion. Central to the argument is the notion that changing the stimulus frequency simply shifts the resulting wave pattern (and thus any nonlinear emission sources) along the basilar membrane. As a consequence of local scaling symmetry, this shift corresponds to a simple frequency rescaling that results in approximate constancy of both $\Delta\theta_{\text{round-trip}}$ and $\Delta\theta_{\text{re-emission}}$. Note, however, that similar arguments should apply to *any* measurement paradigm for which an approximate frequency scaling of the stimulus is maintained.

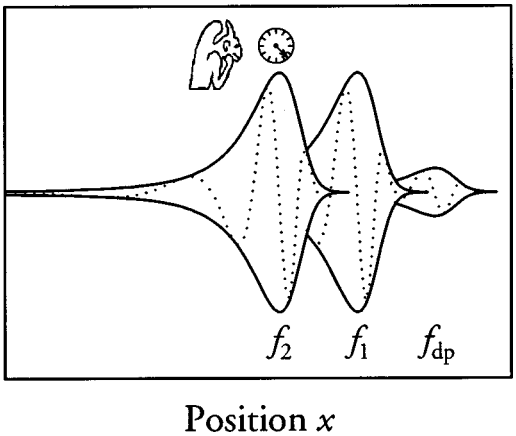

FIG. 8. The demon, responsible here for generating DPOAEs, generates the $2f_1-f_2$ distortion product from his position near the peak of the f_2 traveling wave. When the primary frequency ratio f_2/f_1 is held constant during the frequency sweep, the stimulus and distortion-product wave patterns are simply translated along the cochlear partition. As before, the demon is unable to detect changes in the stimulus frequencies and, consequently, generates a DPOAE with constant phase.

Specifically, the analysis should apply to the generation of distortion-product otoacoustic emissions when the primary-frequency ratio, f_2/f_1, is held fixed (see Fig. 8).[23] When the cochlear position-frequency map is exponential, a constant frequency ratio corresponds to a constant distance along the basilar membrane; the constant ratio f_2/f_1 thus fixes the spatial separations and relative phase relationships (referenced to stapes motion) of the primary traveling waves.[24] So imagine, for example, that the demon—responsible now for generating distortion-products—surfs the peak of the envelope of the f_2 traveling wave. Since the local resonator ticks at a rate proportional to f_2, the demon measures the primary frequencies as f_1/f_2 and 1, values that do not change as the two-tone complex is swept along the cochlea (since the frequency ratio f_2/f_1 is held constant).[25] The analysis thus predicts that for fixed f_2/f_1, the demon emitter should be unable to detect changes in the primary frequencies. Consequently, the resulting emission phase should be roughly constant.

Figure 9 provides a test of this prediction in the human ear. The figure shows the phase of the cubic distortion product $2f_1-f_2$ measured[26] at fixed $f_2/f_1=1.2$. As predicted, the emission phase is essentially independent of frequency,[27] varying by less than half a cycle over most of the nearly three octave range of the figure.[28] In contrast, SFOAE phase measured in the same subject varies by more than 30 cycles over the same frequency range.[29] Measurements in other subjects (total $n=3$) are consistent with these results, and Kemp and Brown have reported similar findings (Kemp and

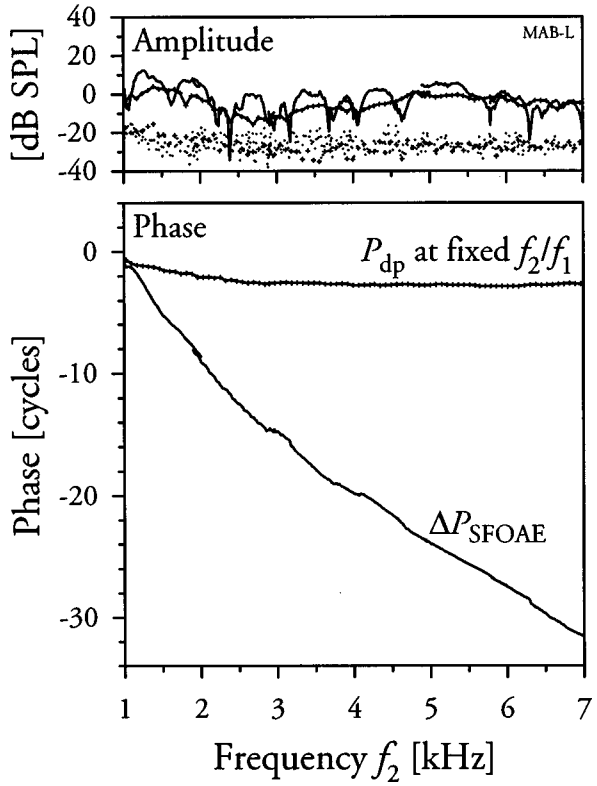

FIG. 9. Constancy of ''frequency-scaled'' DPOAE phase. The solid curves with small crosshairs (+) show the amplitude and phase of P_{dp}, the human $2f_1-f_2$ cubic distortion product measured while holding the ratio of the primary frequencies fixed (at $f_2/f_1=1.2$ with primary levels $\{L_2,L_1\}=\{40,50\}$ dB SPL). With the ratio f_2/f_1 fixed, the primary traveling waves maintain an approximately constant separation along the basilar membrane. To reduce the confounding effects of reflection-source emissions (see Sec. IV C below), the DPOAE was measured in the presence of a 55-dB SPL suppressor tone near $2f_1-f_2$ (e.g., Kemp and Brown, 1983b; Heitmann *et al.*, 1998). (Although the suppressor tone substantially reduced the DPOAE fine structure, it had little effect on the secular variation of the phase important here.) Shown for comparison are measurements in the same subject of ΔP_{SFOAE}, the stimulus-frequency emission obtained using a variant of the suppression method (e.g., Guinan, 1990; Kemp *et al.*, 1990) with probe and suppressor levels of {40,55} dB SPL, respectively. The dotted lines in the upper panel show the approximate measurement noise floor. Note that the data shown here were obtained over several measurement sessions; as a consequence of variations in system calibration, small discontinuities are sometimes visible near session boundaries. Detailed methods for both measurements are presented in the Appendix.

Brown, 1983b; Kemp, 1986). Our abstract thought-experiment thus correctly predicts the striking frequency independence of the phase of emissions generated by frequency-scaled (or ''scaling-symmetric'') nonlinear distortion.[30]

This result supports the argument of Sec. II B—and its contrast with the frequency dependence of echo-emission phase rules out nonlinear distortion as the origin of echo emissions at low levels. If echo emissions and distortion products shared a common origin in cochlear nonlinearity, echo-emission phase, like the phase of $2f_1-f_2$ measured at fixed f_2/f_1, would be essentially independent of frequency. But instead, echo-emission phase rotates rapidly. Contrary to the common view, echo emissions apparently arise by mechanisms fundamentally different from distortion products. When measured with comparable paradigms (i.e., stimuli that preserve the approximate frequency scaling of the stimulus wave pattern characterizing the measurement of stimulus-frequency emissions), echo and distortion-product emissions manifest profound differences in the frequency dependence of their phase that contradict the notion, succinctly expressed by Brass and Kemp (1993), that ''SFOAEs can be thought of as zero-order DPs, and thus as part of the DP series.''

III. ECHO EMISSIONS ARISE BY COHERENT REFLECTION

If echo emissions do not arise by nonlinear distortion, how do they originate? The (mistaken) prediction of the nonlinear-distortion model that $\angle R \approx$ constant hinges on the essential feature that the emission sources move with the wave. The resulting contradiction with experiment suggests that rather than ''surfing'' the wave envelope like the demon, the perturbations that reflect the wave may instead be fixed in space. Thus, rather than being ''re-emitted'' by ''emission generators'' induced through nonlinear distortion, the traveling wave simply scatters off pre-existing irregularities in the mechanics.

The recent theory of coherent reflection filtering (Shera, 1992; Shera and Zweig, 1993b; Zweig and Shera, 1995) characterizes this scattering and indicates that at low stimulus levels echo emissions arise via coherent reflection from the ''random'' impedance perturbations characteristic of cochlear anatomy (Engström *et al.*, 1996; Bredberg, 1968; Wright, 1984; Lonsbury-Martin *et al.*, 1988). Although the impedance perturbations may be densely and randomly distributed along the cochlear partition, the tall, broad peak of the traveling wave localizes the effective scattering to a region spanning the peak of the wave envelope. Most scattered wavelets combine out of phase and cancel one another out. But a simple analog of Bragg's law[31] from x-ray crystallography (Brillouin, 1946) enables a subset of scattered wavelets to combine coherently and form a large reflected wave having the characteristics of echo emissions observed experimentally. In this model, wavelets scattered over an extended region of the cochlea interfere with one another to create a region of coherent reflection that sweeps along the cochlear partition as the frequency is varied. This interference between multiple scattered wavelets precludes the representation of $\angle R$ as a simple sum of phase shifts due to wave propagation and reflection [e.g., along the lines of Eq. (5)]. Nevertheless, the theory predicts that the delay parameter τ—which characterizes the local average phase slope of R in Eq. (4)—equals twice the peak group delay of the basilar-membrane transfer function. Details of the theory, including its many predictions and applications, are presented elsewhere (e.g., Zweig and Shera, 1995; Talmadge *et al.*, 1998a).

IV. DISCUSSION

The arguments we present here demonstrate that the ''common view''—which attributes all otoacoustic emissions, both echo emissions and distortion products, to nonlinear distortion—cannot be correct. Although many argue that otoacoustic emissions share a common origin in co-

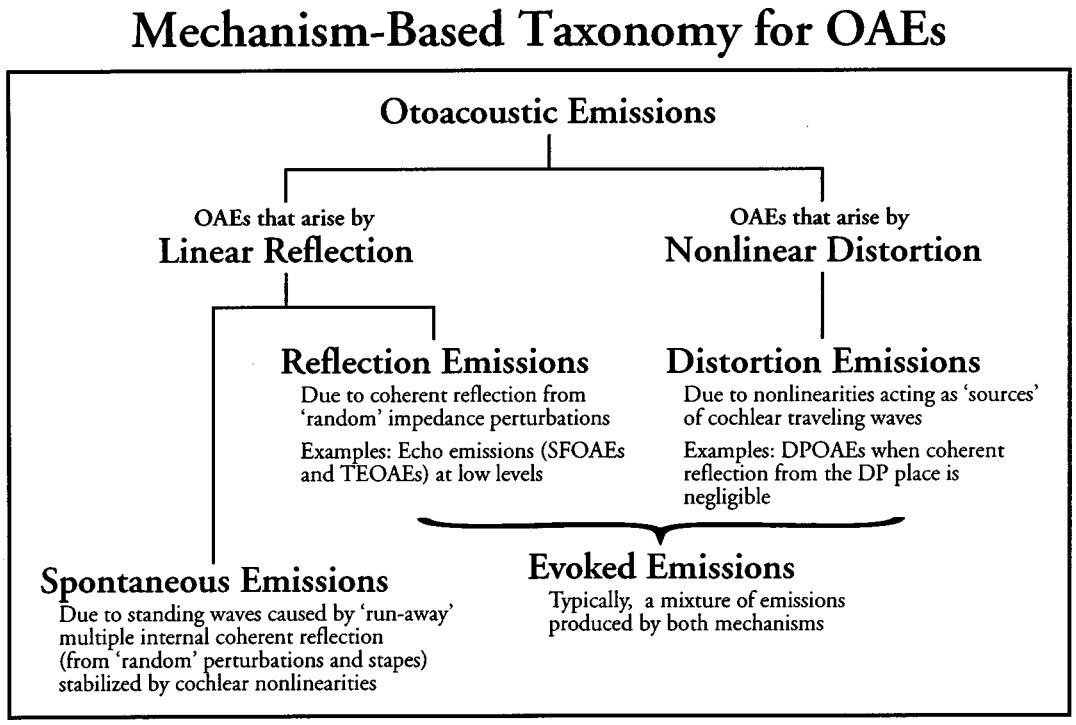

FIG. 10. Proposed mechanism-based taxonomy for mammalian otoacoustic emissions. For conciseness, the names ''reflection-source'' and ''distortion-source'' emissions are here shortened to ''reflection'' and ''distortion'' emissions, respectively.

chlear nonlinearity—that, as Kemp (1997) puts it, ''nonlinearity is at the heart of OAE generation''—we argue that OAEs arise by two fundamentally different mechanisms (i.e., linear coherent reflection[32] versus nonlinear distortion).

A. A mechanism-based taxonomy for otoacoustic emissions

To codify this fundamental distinction we propose a taxonomy for mammalian otoacoustic emissions based on the mechanisms of their generation. This OAE taxonomy, the simplest consistent with current data, is presented in Fig. 10.

Our mechanism-based taxonomy divides evoked otoacoustic emissions into two broad classes:

(i) *Reflection-source emissions*, in which backward-traveling waves arise through the linear (coherent) reflection of forward-traveling waves by pre-existing perturbations in the mechanics (e.g., echo emissions such as SFOAEs and TEOAEs measured at low sound levels); and

(ii) *Distortion-source emissions*, in which backward-traveling waves arise through sources induced by nonlinear distortion (e.g., pure DPOAEs[2]).

Whereas distortion-source emissions would not occur in the absence of cochlear nonlinearities, the coherent reflection responsible for reflection-source emissions is a linear process. The taxonomy is thus consistent with the observations (cf. Fig. 2) that at sound levels near threshold echo-emission amplitude grows linearly with the amplitude of the stimulus (e.g., Kemp and Chum, 1980; Wit and Ritsma, 1979; Wilson, 1980; Zwicker and Schloth, 1984; Shera and Zweig, 1993a) and the principle of superposition holds (Zwicker, 1983). These observations would be more difficult to explain if echo emissions arose through nonlinear distortion.[33]

The conclusion that reflection-source emissions arise through linear coherent reflection may appear to conflict with the well-known level dependence of stimulus-frequency and transiently evoked emissions, which exhibit a nonlinear growth in amplitude at all but the lowest sound levels (cf. Figs. 1 and 2). We emphasize, however, that nonlinear growth with level does not imply that reflection-source emissions arise by a nonlinear process. Rather, the theory of coherent reflection filtering suggests that the nonlinear growth should be understood as a consequence of the level-dependent amplification of forward and reverse traveling waves (Zweig and Shera, 1995), as schematized in Fig. 11. Since the outer hair cells are limited in the forces they can

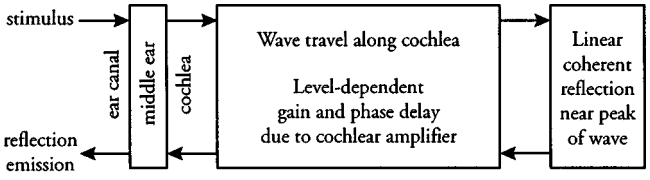

FIG. 11. Simplified conceptual model for the generation of reflection-source emissions. Reflection-source emissions arise from a region of linear coherent reflection near the peak of the traveling-wave envelope. Incident and reflected waves undergo level-dependent gains and phase delays while traveling to, from, and within the scattering reigon. At medium and high stimulus levels, reflection-source emissions therefore exhibit a nonlinear growth with sound level. Note that although they appear separated here for clarity, the regions of coherent reflection and maximal gain overlap within the cochlea. Figure 12 fleshes out this conceptual model (by including phase shifts due to wave propagation) and extends the model to illustrate the mixing of reflection- and distortion-source emissions that occurs during the generation of DPOAEs.

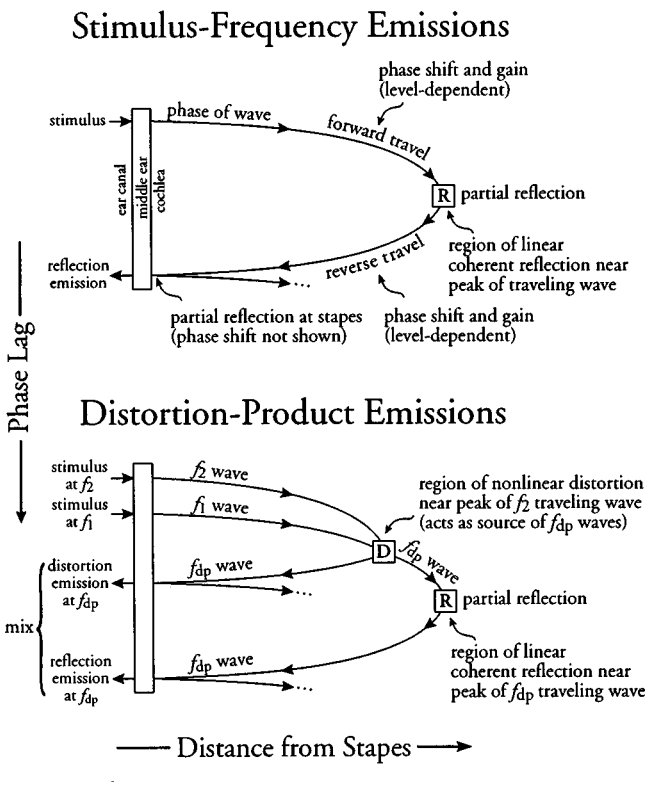

FIG. 12. Schematic diagrams illustrating the generation of stimulus-frequency (top) and distortion-product emissions (bottom) at low sound levels. Both diagrams show phase lags relative to stimulus phase (lag increasing downward) of forward- and backward-traveling waves versus distance from the stapes. At low levels, SFOAEs arise from a region of coherent reflection (**R**) near the peak of the traveling-wave envelope. Stimulus and reflected waves undergo level-dependent gains and phase delays while traveling to and from the scattering region. The generation of low-level DPOAEs is more complicated and involves the mixing of reflection and distortion emissions in the ear canal. A region of nonlinear distortion (**D**) near the peak of the f_2 wave generates waves at frequency f_{dp} that propagate in both directions: The backward-traveling wave propagates to the ear canal as a distortion-source emission; the forward-traveling wave undergoes partial coherent reflection (**R**) near the peak of its wave envelope, generating a second backward-traveling wave that propagates to the ear canal as a reflection-source emission. The DPOAE measured in the ear canal is thus a mixture of emissions arising not just from two spatially distinct regions, but from two fundamentally different mechanisms. Backward-traveling waves arriving at the stapes are partially reflected, creating new forward-traveling waves (arrows with three dots) that subsequently undergo partial coherent reflection themselves. The resulting (infinite) series of multiple internal reflections is truncated for clarity. Note that possible phase shifts due to reflection are not shown.

produce, traveling-wave amplitudes are compressive functions of sound level, with the greatest compression occurring near the peak of the wave envelope, where scattering is maximal. Although the propagation of traveling-wave energy is a nonlinear function of sound level, the physical mechanisms responsible for reversing the direction of that propagation (i.e., coherent reflection from perturbations in the mechanics) are essentially linear.

In our taxonomy, spontaneous emissions are grouped with reflection-source emissions. As originally suggested by Kemp (1980), spontaneous emissions may result from a process of ''run-away'' multiple internal reflection stabilized by cochlear nonlinearities. In the view espoused in the taxonomy, multiple cycles of propagation, amplification, and coherent reflection[34] create narrow-band cochlear standing waves measurable in the ear canal (Zweig and Shera, 1995; Talmadge and Tubis, 1993; Talmadge *et al.*, 1997).

When we argue that reflection- and distortion-source emissions arise by different mechanisms, we mean that the processes responsible for creating backward-traveling waves differ for the two emission types. For example, although the backward-traveling waves created by nonlinear distortion may arise, at least in part, through the action of nonlinear cellular demons (OHCs) pushing and pulling on the basilar membrane, reflection-source emissions do not result directly from OHC forces. Rather, we argue that reflection-source waves arise by the linear, ''passive'' scattering of the forward-traveling wave off more or less random perturbations in the mechanics. Although the waves created by this scattering may then be amplified through the collective action of the ''cochlear amplifier,'' the backward-traveling waves themselves are not fundamentally the product of nonlinear force generation by outer hair cells.

Once generated, however, backward-traveling waves produced by either mechanism propagate basally to the stapes (from which they may be partially reflected), through the middle ear, and out into the ear canal. While propagating, emissions of both types undergo delays, phase shifts, and gains (e.g., due to the cochlear amplifier or reverse middle-ear transmission), as illustrated in Fig. 12. Thus, although their mechanisms of generation are fundamentally different, both emission types traverse a similar pathway on their way to the ear canal, and both are potentially vulnerable to modifications or disruptions of this pathway (e.g., to changes in outer-hair-cell function, middle-ear transfer characteristics, etc.). Although a common dependence on propagation pathways from cochlea to ear canal presumably introduces correlations in reflection- and distortion-source emission amplitude, the taxonomy emphasizes that their respective mechanisms of generation—and hence their dependence on underlying parameters of cochlear mechanics—remain fundamentally distinct.

Although identifying what we suggest are the two principal branches of the OAE family tree, our taxonomy makes no attempt to adumbrate the sub-branches. For example, in some species (e.g., rodents and rabbits), considerable evidence suggests that distortion-source emissions can be usefully divided into subtypes, conventionally designated the ''active or low-level component'' and the ''passive or high-level component'' (e.g., Norton and Rubel, 1990; Mills and Rubel, 1994; Whitehead *et al.*, 1992a,b, 1995; Whitehead, 1998).[35] The differential vulnerability of these two distortion components to physiological insult suggests that they arise from different mechanisms within the cochlea.[36] And although coherent reflection from ''random'' mechanical perturbations appears to be the dominant reflection mechanism in the normal primate ear, reflection by other mechanisms may contribute in some circumstances. For example, incoherent reflection from large punctate perturbations may dominate in certain pathologies or in specialized cochleae, such as in the ''auditory fovea'' of the CF-FM bat (e.g., Kössl and Vater, 1995), in which the mechanical properties of the cochlear partition change rapidly with position. When

coupled with knowledge of the underlying mechanisms, a more complete identification of the different emission subtypes could presumably prove of considerable value in the application of OAEs to noninvasive diagnostics.

B. Relation to the conventional classification of OAEs

As the taxonomy implies, we argue that backward-traveling waves originating by coherent reflection and nonlinear distortion constitute the elemental OAE ''building blocks'' that combine to form evoked emissions measured in the ear canal (i.e., echo emissions and DPOAEs). In any given measurement, the two types mix in varying degrees dependent on the species, the stimulus parameters, and the state of the cochlea. For example, although presumably arising largely by coherent reflection, echo emissions measured at medium and high stimulus levels may contain significant energy from distortion-source waves created by nonlinear distortion (e.g., Yates and Withnell, 1998; Withnell and Yates, 1998).

The OAE taxonomy thus provides a mechanism-based alternative to the conventional classification scheme, which classifies emissions based principally on the stimuli used to elicit them (e.g., TEOAEs, SFOAEs, and DPOAEs). *The mixing of reflection- and distortion-source emissions in the ear canal precludes any fixed correspondence between the two schema*. At low levels, however, echo emissions (i.e., TEOAEs and SFOAEs) arise predominantly through linear coherent reflection. And under circumstances when coherent reflection from the f_{dp} place can be neglected, DPOAEs arise predominantly from distortion-source waves due to nonlinear distortion. Thus, in these special cases, the division of evoked emission into ''echo emissions'' and ''distortion products''—a division made at the beginning of this paper based on the relative spectral content of the stimulus and the emission—corresponds to a fundamental difference in generation mechanism as well.[37] As commonly measured, however, evoked OAEs typically represent mixtures of the different emission types. We therefore find the conventional, stimulus-based emission nomenclature more confusing than helpful for understanding the origin and properties of OAEs.

C. An example of reflection- and distortion-source mixing

Our taxonomy and its identification of the fundamental OAE ''building blocks'' provides a framework that simplifies the often bewildering complexity of OAE phenomenology. The phenomenon of DPOAE fine structure, for example, can be understood in terms of the mixing of the two OAE ''building blocks.'' As originally suggested by Kim (1980), much of DPOAE fine structure apparently arises through the interference of two distinct sources located near the f_2 and f_{dp} places (e.g., Kim, 1980; Kemp and Brown, 1983b; Shera and Zweig, 1992). Although the ''two-source'' model for DPOAEs now appears well established (e.g., Gaskill and Brown, 1990; Brown *et al.*, 1996; Engdahl and Kemp, 1996; Brown and Beveridge, 1997; Talmadge *et al.*, 1997, 1998b; Heitmann *et al.*, 1997, 1998; Fahey and Allen, 1997; Siegel *et al.*, 1998), our taxonomy goes further and identifies these two sources as arising not simply from two distinct locations, but from *two different mechanisms*: a distortion source near the f_2 place and a coherent reflection from the f_{dp} place. (The combined process is illustrated in the bottom panel of Fig. 12, where the distortion- and reflection-source regions are denoted **D** and **R**, respectively.) Indeed, as our argument demonstrates for the frequency-scaled, fixed-f_2/f_1 paradigm, it is fundamentally this difference in emission-source *mechanism*—and *not*, as is often implied (e.g., Brown *et al.*, 1996), the difference in source *location*—that is ultimately responsible for the different frequency dependencies of the phase of the emissions arising from the two interfering sources. Thus, as commonly measured, *DPOAEs actually comprise a mixture of backward-traveling waves that arise by two fundamentally different mechanisms within the cochlea*. By matching measurements of DPOAE fine structure with predictions obtained using the model of coherent reflection filtering, Talmadge *et al.* (1999) provide elegant experimental corroboration of these ideas.

The relative mix of the two OAE ''building blocks'' measured in the ear canal presumably depends on stimulus parameters such as frequency and level. For example, Fig. 12 predicts that variations in the DPOAE mix should occur as a consequence of any change in the relative amplitudes of the net forward- and backward-traveling distortion-source waves emanating from **D**. Mechanisms that may produce such changes include suppression by the primaries (e.g., Kanis and de Boer, 1997; Shera and Guinan, 1997), nonlinearities in the effective forward and reverse ''load impedances'' (Shera and Zweig, 1991, 1992; Fahey and Allen, 1997), and phase-dependent interference between distortion-source wavelets within the DP source region (e.g., van Hengel, 1996; Neely and Stover, 1997; Kemp and Knight, 1999). Variations in the relative mix would also be expected as a result of any mechanism (e.g., suppression) that affects the cochlear amplifier in the region between **D** and **R** and thereby modifies the strength of the reflection-source emissions that scatter back from **R** (e.g., Kemp and Brown, 1983b; Kummer *et al.*, 1995; Heitmann *et al.*, 1998).

Several studies can be interpreted in this light as providing evidence for stimulus-dependent mixing. For example, the data of Fahey and Allen (1997) in cat suggest that the relative amplitude of the distortion- and reflection-source components varies with the primary level ratio, L_2/L_1. Similarly, Kemp's (1986) measurements in human ears suggest a dependence on the ratio f_2/f_1. At values of f_2/f_1 relatively close to one ($f_2/f_1 \lesssim 1.1$), the frequency dependence of the $2f_1-f_2$ DPOAE shows regular variations (nulls) in amplitude and a more rapidly rotating phase distinctly different from the nearly constant amplitude and phase obtained at larger values of f_2/f_1 (cf. Fig. 9). These features appear consistent with the view that the measured DPOAE arises from a variable f_2/f_1-dependent mix of waves from two distinct sources, and, furthermore, that these two sources—in accordance with their respective identities as sources of nonlinear distortion and coherent reflection—produce emissions with very different frequency dependence in their phase. Applying the reasoning of Sec. II B to emissions evoked by any frequency-scaled stimulus (e.g., fixed

f_2/f_1), we hypothesize that (1) a nearly frequency-independent phase implies that the OAE arises mainly by nonlinear distortion, whereas (2) a rapidly rotating phase implies that the OAE arises mainly by coherent reflection.

D. The taxonomy resolves OAE ''paradoxes''

The taxonomy provides a conceptual framework that helps resolve issues that appear paradoxical if all emissions are regarded as sharing a common origin in nonlinear distortion. For example, consider the observations that

(i) whereas primates tend to have large SFOAEs and TEOAEs, many SOAEs, and small DPOAEs, rabbits and guinea pigs have the relative amplitudes and/or prevalence of these emissions reversed (e.g., Zurek, 1985; Whitehead *et al.*, 1996a); and

(ii) whereas SFOAEs and SOAEs are abolished by aspirin administration, DPOAEs can remain almost unchanged (e.g., Martin *et al.*, 1988; Wier *et al.*, 1988).

In the common view these observations are largely unintelligible and, indeed, are often presented as paradoxes. For if all emissions shared a common origin in cochlear nonlinearity, their relative amplitudes would be expected to vary together, both between species and in response to aspirin or other ototoxic drugs.[38] Our taxonomy resolves these ''paradoxes'' by recognizing fundamental differences in the mechanisms of OAE generation. As shown below, when differences in their mechanisms of generation are taken into account, the observation that the different emission types can be ''decoupled,'' both between species and by certain experimental manipulations and/or pathologies, is no longer surprising (indeed, it is predicted).

First, consider species differences in OAE amplitude and prevalence. Whereas distortion-source emissions depend on the form and magnitude of cochlear nonlinearities (e.g., on the effective ''operating point'' along hair-cell displacement-voltage transduction functions), reflection-source emissions depend strongly on the size and spatial arrangement of micromechanical impedance perturbations (e.g., on variations in hair-cell number and geometry). In the light of these different dependencies, species differences between the two emission types no longer appear mysterious: They simply reflect differences across species in the respective factors underlying emission generation. Indeed, the theory of coherent reflection filtering provides an interesting hypothesis to explain the striking species differences in reflection-emission amplitudes (Zweig and Shera, 1995): The model predicts that disorderly patterns of impedance perturbations produce large reflections whereas orderly patterns produce only small reflections.[39] Correspondingly, in contrast to the cellular disorder characteristic of the primate organ of Corti, anatomical regularity constitutes an ''impressive feature'' of the rodent cochlea (e.g., Wright, 1984). Thus, the theory of coherent reflection filtering accounts naturally for the relative amplitudes of reflection emissions in humans (large) and guinea pig (small).[40]

Next, consider the effects of aspirin on OAEs. Once reflection- and distortion-source emissions are understood as separate emission types, a number of possible explanations for their differential responses arise. For example, the experiments of Martin *et al.* (1988) suggest that aspirin may somehow reduce the gain of the cochlear amplifier while preserving the nonlinearities responsible for generating distortion emissions. Although a reduction in the gain of the cochlear amplifier would be expected to have a dramatic effect on reflection emissions—which arise from scattering near the peak of the traveling wave, where the gain is presumably largest—the effect on distortion-source emissions could be significantly less. To see this, note that suppression studies indicate that distortion-source waves appear to be generated predominantly in the region of maximum overlap between the primaries near the peak of the f_2 traveling wave (e.g., Brown and Kemp, 1984; Kummer *et al.*, 1995). The region of nonlinear distortion (**D** in Fig. 12) is therefore often significantly basal to the f_{dp} place (near **R**). For example, the generation of cubic distortion products at the frequency $f_{dp}=2f_1-f_2$ at a primary-frequency ratio of $f_2/f_1\approx 1.25$ occurs at the frequency ratio $f_{dp}/f_2\approx 0.6$, corresponding to roughly three-quarters of an octave. At the low and medium sound-pressure levels for which the amplifier gain is significant, this frequency ratio corresponds to a distance from the f_{dp} place larger than the width of the traveling-wave envelope.[41] Thus, the distortion source lies basal to the region of maximal gain for the f_{dp} traveling wave (see Fig. 12), and, consequently, the backward-traveling distortion-source wave experiences relatively little amplification as it travels to the stapes. The resulting DPOAE would thus appear relatively insensitive to the gain of the cochlear amplifier at the distortion-product frequency.[42]

Note, however, that the analysis is complicated by possible mixing of the emission types, specifically by contributions to the measured DPOAE from reflection-source emissions scattered back from the f_{dp} place. Although aspirin may have little effect on the distortion source (**D**), the argument outlined above predicts a decrease in the magnitude of any concomitant reflection-source emissions (due to reductions in the f_{dp} amplifier gain near **R**) and thus significant changes in the resulting distortion-product microstructure. Unfortunately, the measurements reported by Martin *et al.* do not permit an evaluation of this prediction.[43] Nevertheless, the general idea that reflection-source emissions may be more sensitive to changes in the f_{dp} amplifier gain is consistent with the observation that the emission component from the f_{dp} place (i.e., the coherent reflection) is differentially diminished by presumed reductions in the amplifier gain due to efferent feedback evoked by contralateral noise (Brown and Beveridge, 1997).

E. Implications of the taxonomy for the use of OAEs

As a consequence of their different origins, reflection- and distortion-source emissions presumably manifest different dependencies on cochlear pathologies. However, the mixing of the two emission types confounds an understanding of their individual characteristics and clouds the assessment of their different utilities as clinical diagnostic and screening aids. As a result, it is of considerable theoretical and practical interest to isolate and characterize the properties of each emission type (and related subtypes) separately,

to understand the factors that control their mixing, and to determine their individual correlations with cochlear pathology.

Although some degree of mixing among the OAE ''building blocks'' may prove unavoidable, several existing measurement techniques hold promise for at least partially separating the two types of emissions. For example, reflection-source emissions can be studied at low sound levels using methods that do not cancel the low-level linear components of the response (e.g., Kemp and Chum, 1980; Shera and Zweig, 1993a). And in DPOAE measurements, the confounding contributions of reflection-source emissions can be substantially reduced by using a third primary tone with frequency near f_{dp} to suppress amplification of the reflection-source emissions that scatter back from this location (e.g., Kemp and Brown, 1983b; Heitmann *et al.*, 1998). Alternatively, the reflection- and distortion-source components of DPOAEs may be separable based on onset latency, either in the time (e.g., Whitehead *et al.*, 1996b; Talmadge *et al.*, 1998b) or the frequency domain (e.g., Brown *et al.*, 1996). Note that extracting or suppressing individual components of an evoked emission may be more difficult—and problems of interpretation correspondingly greater—when the respective regions of wave generation [e.g., the regions of nonlinear distortion (**D**) and coherent reflection (**R**) in Fig. 12] overlap extensively within the cochlea. For DPOAEs, significant overlap can be expected when using primary-frequency ratios close to one.

Our taxonomy predicts that reflection- and distortion-source emissions—when properly separated and studied—will manifest considerable differences in their correlations with particular cochlear pathologies. Clinical measurement of both types of evoked emissions will presumably be needed to maximize the power and specificity of OAEs as noninvasive probes of cochlear function.

ACKNOWLEDGMENTS

We gratefully acknowledge many stimulating discussions with Jont B. Allen, Paul F. Fahey, David T. Kemp, Nelson Y. S. Kiang, Stephen T. Neely, Sunil Puria, Carrick L. Talmadge, and George Zweig and thank John R. Iversen, M. Charles Liberman, William T. Peake, John J. Rosowski, and three anonymous reviewers for their helpful critical readings of and comments on the manuscript. The work was supported by NIDCD/NIH Grant Nos. DC00108, DC03494, DC00119, and DC00235.

APPENDIX: MEASUREMENT METHODS

This appendix outlines the methods used to obtain the distortion-product and stimulus-frequency emission data shown in Fig. 9. All measurements were performed with subjects comfortably reclined in a sound-proofed, vibration-isolated chamber (Ver *et al.*, 1975), well shielded from sources of electrical interference (Golka, 1994). Stimulus waveforms were generated and responses acquired and averaged digitally using a Spectrum Signal Processing PC/C31 DSP board with two Burr-Brown analog daughter modules providing eight channels of synchronized analog I/O. The hardware was computer controlled using a custom data-acquisition system implemented in LabVIEW and supplemented with hand-coded time-domain artifact-rejection and synchronous-averaging routines. Acoustic signals were transduced at sampling rates of 59.94 kHz using a calibrated Etymotic Research ER-10c DPOAE probe system supplemented with an ER-3A earphone whose sound-delivery tube was threaded through the ER-10c foam ear-tip. Measurement frequency resolution was always sufficient to resolve ambiguities due to phase unwrapping. Control experiments in a small cavity indicated that the measurement-system distortion was at or below the noise floor (typically less than -25 dB SPL). Treatment of human subjects was in accordance with protocols approved by the Human-Studies Committee at the Massachusetts Eye and Ear Infirmary.

Measurement of DPOAEs: To reduce reflection-source contributions to the measured emission (see Sec. IV C), DPOAEs were measured in the presence of a suppressor tone with frequency near $2f_1-f_2$ (e.g., Kemp and Brown, 1983b; Heitmann *et al.*, 1998). Although the suppressor tone substantially reduced the DPOAE fine structure, it had little effect on the more secular variation of the phase of primary interest in the context of this paper.

At each measurement frequency the acoustic stimulus had the form

$$\text{stimulus}=\underbrace{\langle XX\ldots X\rangle}_{\#\geqslant M}, \tag{A1}$$

where X represents a periodic 4096-sample ($\approx$68.33 ms) segment containing an integral number of periods of the stimulus waveform. The waveform consisted of three frequency components: a component at each of the two primary frequencies, f_1 and f_2, and a third component at the suppressor frequency, f_s, near $2f_1-f_2$. The phase of each component was adjusted to produce an upwards zero-crossing (sine-phase) at the beginning of each X segment. The respective stimulus levels $\{L_1,L_2,L_s\}$ were {50,40,55} dB SPL. To minimize artifactual distortion, the three component waveforms were delivered synchronously through separate earphones.

Measurements were made versus frequency by sweeping f_2 from high frequencies to low while varying f_1 to keep the primary-frequency ratio at the fixed value $f_2/f_1=1.2$. The suppressor frequency was also swept, with $f_s=2f_1-f_2+\Delta f_s$ and $\Delta f_s=43.9$ Hz.[44] The periodic segments X were presented repeatedly until a total of $M=32$ corresponding artifact-free responses[45] were collected; at each frequency the total stimulus duration was therefore $\geqslant 32\times 68.33$ ms $\approx$2.2 s. To reduce unwanted transients the waveform was ramped on and off by pre- and postpending two additional segments (indicated by the angled brackets $\langle$ and $\rangle$) with envelopes of half Blackman windows with 2.5-ms rise and fall times. After digitizing the resulting ear-canal pressure, responses to the segments X were averaged and the amplitude and phase of the $2f_1-f_2$ distortion component extracted using Fourier analysis.

Measurement of SFOAEs: Stimulus-frequency emissions were measured using a variant of the suppression method

(e.g., Guinan, 1990; Kemp *et al.*, 1990; Brass and Kemp, 1991, 1993; Souter, 1995). In this method, the emission is obtained as the complex (or vector) difference between the ear-canal pressure at the probe frequency measured first with the probe tone alone and then in the presence of a stronger suppressor tone at a nearby frequency.

At each measurement frequency the acoustic stimulus had the form

$$\text{stimulus} = \underbrace{\langle XX\ldots X\rangle}_{\#\geqslant M}, \tag{A2}$$

where X represents a periodic (5×4096)-sample ($\approx$341.66 ms) segment consisting of two components:

$$X = \begin{cases} \pi_1\Pi_2\Pi_3\pi_4\pi_5\Pi_6\Pi_7\pi_8 & \text{(probe earphone)}, \\ o_1O_2O_3\langle_4\sigma_5\Sigma_6\Sigma_7\rangle_8 & \text{(suppressor earphone)}. \end{cases} \tag{A3}$$

Each component consisted of four long (uppercase) and four short (lowercase and angled brackets) intervals. The long intervals were each 4096 samples ($\approx$68.33 ms) in duration and contained an integral number of periods of the probe (Π_i), suppressor (Σ_i), and zero (O_i) waveforms, respectively. The short intervals were one-fourth the duration of the long intervals (i.e., 1024-samples or $\approx$17.08 ms) and did not, in general, contain an integral number of periods of the corresponding waveform. The short intervals π_i, σ_i, and o_1 allowed for response settling time and contained segments of the probe, suppressor, and zero waveforms, respectively. The short intervals $\{\langle_4,\rangle_8\}$ were used to ramp the suppressor tone {on,off} using the {first,second} half of the Blackman window. The two components of X were synchronized and presented simultaneously through separate earphones. Note that whereas the probe tone played continuously during the measurement, the suppressor tone cycled on and off repeatedly due to alternation of the zero and suppressor waveforms. The probe and suppressor levels $\{L_p,L_s\}$ were {40,55} dB SPL.

Measurements were made versus probe frequency by sweeping both probe and suppressor from high frequencies to low, with $f_s=f_p+\Delta f_s$ and $\Delta f_s=43.9$ Hz. The periodic segments X were played repeatedly until a total of $M=64$ corresponding artifact-free responses were collected; at each frequency the total stimulus duration was therefore $\geqslant64\times341.66$ ms$\approx$22 s. To reduce unwanted transients the probe waveform was ramped on and off by pre- and postpending two additional segments [indicated by the angled brackets $\langle$ and $\rangle$ in Eq. (A2)] with envelopes of half Blackman windows with 2.5-ms rise and fall times. After digitizing the resulting ear-canal pressure, responses to all probe-alone segments (i.e., all segments Π_2 and Π_3) were averaged to form Y_p; similarly, the responses to all probe+suppressor segments (i.e., all segments Π_6 and Π_7) were averaged to form Y_{p+s}. From these averaged response waveforms, the complex amplitudes of the f_p components of the ear-canal pressure, denoted $P_p(f_p)$ and $P_{p+s}(f_p)$, were extracted using Fourier analysis. The complex quantity $\Delta P_{SFOAE}(f_p)$ was then defined as

$$\Delta P_{SFOAE}(f_p) \equiv P_p(f_p) - P_{p+s}(f_p)e^{-2\pi i\Delta N\Delta T f_p}, \tag{A4}$$

where the complex exponential compensates for the phase shift in the probe due to the time interval, $\Delta N\Delta T$, between the probe-alone and probe+suppressor segments. Here, ΔT is the sampling interval (reciprocal of the sampling rate), and ΔN represents the total number of these intervals that separate the two segments:

$$\Delta N = \#\text{ samples } (\Pi_2\Pi_3\pi_4\pi_5) = 2\tfrac{1}{2}\times4096 = 10\,240. \tag{A5}$$

Note that when the two segments are separated by an integral number of periods of the probe waveform, the phase shift modulo 2π is zero.

Due to the long averaging time and high-frequency resolution (the probe frequency was typically decremented in steps of approximately 15 Hz), Fig. 9 shows data obtained over several measurement sessions. Unwrapped phase curves from the different sessions were patched together by shifting them vertically by integer multiples of 2π to obtain a (nearly) continuous curve. As a consequence of variations in system calibration, small discontinuities are sometimes visible in both amplitude and phase at the ''seams'' near session boundaries.

[1]In the common view, stimulus-frequency emissions (SFOAEs) are regarded as ''zeroth-order'' distortion-products (DPOAEs) produced by the degenerate primary stimulus pair $f_1=f_2$ (e.g., Brass and Kemp, 1993; Kemp, 1998). Patuzzi (1996), for example, argues this point from an operational perspective:

> ''The nonlinear growth of ear canal sound pressure with stimulus level is easily explained by a nonlinear input admittance to the ear canal, due to the nonlinear input admittance of the cochlea. Because the sound level in the ear canal does *not* scale proportionately with the stimulus level, the sound level predicted at low stimulus levels on the basis of linear extrapolation from high stimulus levels does not agree with that actually measured. The difference between the expected and measured acoustic waveforms is often attributed to the presence of a 'stimulus frequency OAE,' when it is just as easily explained by a nonlinear cochlear input admittance and an error of extrapolation. The measurement of SFOAEs can be viewed as an analysis of the first harmonic of the nonlinear input admittance. [...] Just as the SFOAEs represent the nonlinear growth of the first harmonic of the cochlear input admittance, the DPOAEs can be viewed as two-tone interactions due to the nonlinearity of the cochlear input admittance.''

[2]We use the qualifier ''pure'' here because distortion products measured in the ear canal are often *mixtures* of emissions generated by both distortion- and reflection-source mechanisms. We elaborate on this point in Sec. IV below.

[3]A preliminary account of this work has been presented elsewhere (Shera and Guinan, 1998).

[4]In this paper, we focus on acoustically evoked otoacoustic emissions; emissions evoked by direct electrical stimulation of the organ of Corti are not considered.

[5]In a normal ear, the threshold hearing curve often manifests corresponding peaks and valleys (e.g., Elliot, 1958; Thomas, 1975; Long, 1984); at levels near threshold, a swept tone of constant driver level moves alternately into and out of perception (e.g., Kemp, 1979b; Cohen, 1982).

[6]The symbol ''$\equiv$'' denotes equivalence—it means that the quantity on the left (in this case, the cochlear reflectance) is defined by the quantity on the right (here, the complex ratio of forward- and backward-traveling pressure waves at the stapes).

[7]Although we later conclude that the terminology is physically appropriate, the term ''reflectance'' should not be understood to imply any tacit assumption of a particular emission mechanism.

[8]Equation (2) neglects terms proportional to $R^2, R^3, \ldots$ that arise due to multiple internal reflection within the cochlea (see Shera and Zweig, 1993a; Zweig and Shera, 1995). See also Fig. 12 of this paper.

[9]A wider range of emission data from humans (Shera and Zweig, 1993a) shows that there exist extended frequency regions well characterized by statements (3) punctuated by short ''anomalous regions'' in which the re-

flectance varies more rapidly (see also Fig. 9 and footnote 29).

[10]Over a wider frequency range, R varies roughly as

$$R \approx R_0 e^{-2\pi i N \ln(f/f_{\max})},$$

where $f_{\max}$ is the maximum frequency of hearing. Except near ''anomalous regions'' (see footnote 9), both the complex amplitude R_0 and the dimensionless parameter N generally vary slowly with frequency (Shera and Zweig, 1993a). By expanding $\angle R$ in a power series about an arbitrary reference frequency one can show that the effective ''delay,'' τ, appearing in Eq. (4) varies inversely with frequency as $\tau(f) = N/f$. The parameter N thus represents the delay measured in units of the stimulus period.

[11]For simplicity, we have ignored dispersive effects due to sound transmission through the middle ear. The echo described here is that which would be measured at the basal end of the cochlea near the stapes (i.e., at the point where the reflectance R is defined).

[12]We wish to compare the observed change in $\Delta\theta_{\text{forward}}$ with the value predicted using the assumption that $\angle R \approx 2\Delta\theta_{\text{forward}}$. [The factor of 2 arises from round-trip travel; see Eq. (7).] The change, $\Delta\{\angle R\}$, in the phase of R over the frequency interval Δf_{cf} between the characteristic frequencies of the two measurement points can be estimated as follows. Since $\angle R$ rotates through 2π radians over the interval Δf_{OAE} between spectral maxima, the interval Δf_{cf} between the characteristic frequencies of the two measurement points corresponds to a phase shift of roughly

$$\Delta\{\angle R\} \approx 2\pi \Delta f_{\text{cf}} / \Delta f_{\text{OAE}}.$$

Unfortunately, the frequency spacing Δf_{OAE} between emission spectral maxima has not been measured in the squirrel monkey. However, measurements of SFOAEs at frequencies of 1–2 kHz in the rhesus monkey (Lonsbury-Martin *et al.*, 1988) indicate that $\Delta f_{\text{OAE}}/f \approx \frac{1}{13}$—compared with roughly $\frac{1}{15}$ at similar frequencies in humans (Shera and Zweig, 1993a)—suggesting that species differences may be small among primates. Using the human value yields

$$\Delta\{\angle R\} \approx 2\pi 15 \Delta f_{\text{cf}}/f_{\text{cf}} \approx 6\pi,$$

where the ratio $\Delta f_{\text{cf}}/f_{\text{cf}} \approx |f_{\text{cf}}(x_1) - f_{\text{cf}}(x_2)| / \sqrt{f_{\text{cf}}(x_1) f_{\text{cf}}(x_2)} \approx \frac{1}{5}$ has been estimated from the data in Fig. 5. Under the assumption that $\angle R \approx 2\Delta\theta_{\text{forward}}$, the predicted change in $\Delta\theta_{\text{forward}}$ is $\frac{1}{2}\Delta\{\angle R\}$ (i.e., approximately 3π, as shown by the scale bar in Fig. 5). Note that human emission measurements suggest that the ratio $\Delta f_{\text{OAE}}/f$ decreases at higher frequencies (Zweig and Shera, 1995); our calculation based on the value of $\Delta f_{\text{OAE}}/f$ near 1 kHz may therefore underestimate the value of $\Delta\{\angle R\}$ at 6 kHz.

Alternatively, the value of $\Delta\{\angle R\}$ can be estimated directly from the data in Fig. 5 using the theory of coherent reflection filtering (see Sec. III), which predicts the relation $\Delta f_{\text{OAE}}/f \approx 1/2f\tau_{\text{group}}$, where τ_{group} is the transfer-function group delay measured at the characteristic frequency (Zweig and Shera, 1995). Calculating the slope of the transfer-function phase from the data in Fig. 5 yields the value $\Delta f_{\text{OAE}}/f \approx \frac{1}{8}$, an estimate that implies a value of $\Delta\{\angle R\}$ roughly half that obtained above. Because the transfer-function phase varies more rapidly when the amplitude response is sharper, the estimates of τ_{group} and $\Delta\{\angle R\}$ obtained here from Fig. 5 presumably underestimate the values characteristic of healthy preparations at low sound levels (cf. Zweig and Shera, 1995).

The obvious uncertainty in these various estimates notwithstanding, the value of $\Delta\{\angle R\}$ consistently appears many times greater than the observed change in $\Delta\theta_{\text{forward}}$.

[13]Direct determination of phase shifts due to reverse propagation may now be possible using careful measurements of OAEs evoked by focal electrical stimulation of the cochlear partition (e.g., Nakajima *et al.*, 1994, 1999).

[14]For nice reviews, see the series by de Boer (1980, 1984, 1991).

[15]Even if $\Delta\theta_{\text{forward}}$ and $\Delta\theta_{\text{reverse}}$ are not numerically equal, the constancy of $\Delta\theta_{\text{round-trip}}$ follows so long as $\Delta\theta_{\text{reverse}} \approx$ constant, as expected in an approximately scaling-symmetric cochlea.

[16]Our thought experiment alludes, of course, to ''Maxwell's demon'' (e.g., Maxwell, 1871; Leff and Rex, 1990), a ''very observant and neat-fingered being'' invented by Maxwell to illustrate the statistical character of the second law of thermodynamics. Compared to Maxwell's demon, our demon is rather myopic, but is capable of doing work.

[17]The demon's phase formula may depend not only on the frequency of basilar-membrane vibration, but also on its local amplitude. We focus here, however, on changes in stimulus frequency and assume, for simplicity, that the stimulus amplitude is held constant during the measurement (e.g., as it was during the frequency sweeps shown in Fig. 1).

[18]Of course, the demon must also determine, from his measurements of basilar-membrane displacement, how *hard* he must push in order to generate an emission with the correct relative amplitude, $|R|$.

[19]Despite an aptitude for pushing and pulling, the demon is no omniscient or omnipotent being. Rather, the demon is but a stand-in for unspecified biophysical mechanisms and, consequently, must make do with the tools he finds at hand.

[20]Every transverse section of the cochlear partition may exhibit, in addition to the macromechanical oscillator tuned to f_{cf}, various micromechanical oscillators, modes of vibration, or other processes with different resonant frequencies and/or characteristic time scales (e.g., tectorial-membrane resonances, membrane time constants, efferent feedback signals, etc.). At each location, the cochlear partition may therefore contain not one but multiple ''clocks;'' and these multiple clocks could, in principle, be arranged to enable the demon to detect changes in the stimulus frequency. However, so long as the emission process does not depend sensitively on the relative values of these additional resonant frequencies [e.g., because the micromechanical oscillators have nearly the same spatial dependence as $f_{\text{cf}}(x)$ (e.g., Allen and Fahey, 1993) and/or because the relevant time scales are either much larger or much smaller than $1/f_{\text{cf}}$], then each location along the cochlear partition can effectively be regarded as having a single independent clock. At low and moderate sound levels, this assumption is supported both by the existence of scaling symmetry and, most compellingly, by the measurements of emission phase presented in Sec. II C. These measurements suggest that even if additional clocks exist, the demon (i.e., the source of nonlinear distortion) does not consult them while generating distortion-product emissions.

[21]With no loss of generality we can take the proportionality constant to be unity.

[22]More precisely, the demon cannot generate backward-traveling waves with a phase shift that depends *reproducibly* on frequency. The demon could, however, generate a stochastic frequency dependence by pushing and pulling on the basilar membrane at random. Such a strategy would, of course, be at odds with the repeatability of the emission measurements.

[23]In the nonlinear-distortion model, stimulus-frequency emissions simply correspond to the limiting case $f_2/f_1 = 1$.

[24]A constant ratio f_2/f_1 fixes not only the spatial separation between the envelopes of the primary traveling waves, but also the distances between all resulting distortion-product waves whose frequencies fall in the exponential portion of the cochlear map. *Proof*: If $\alpha \equiv f_2/f_1 =$ constant, then

$$f_{\text{dp}}/f_2 = (nf_1 - mf_2)/f_2 = n/\alpha - m = \text{constant},$$

for all values of n and m.

[25]For simplicity, we have assumed here that the demon is able to separate the complex temporal waveform of basilar-membrane vibration into its component frequencies. To the demon sitting at the f_2 place, the two-tone complex might look like a sinusoid of frequency $\frac{1}{2}(1 + f_1/f_2)$, amplitude modulated at the frequency $\frac{1}{2}(1 - f_1/f_2)$, where frequencies are measured in the demon's local units (i.e., in units of f_2).

[26]Measurement methods are detailed in the Appendix.

[27]The near constancy of ''frequency-scaled'' DPOAE phase differs from the more rapid phase rotation obtained when DPOAEs are measured using a stimulus paradigm (e.g., fixed f_1, fixed f_2, or fixed $2f_1 - f_2$) for which the cochlear wave pattern is not simply translated along the cochlear partition (e.g., Kimberley *et al.*, 1993; O Mahoney and Kemp, 1995). The strong dependence of the observed phase gradient on the measurement paradigm argues against any naive equivalence between DPOAE phase gradients and ''wave travel times'' within the cochlea.

[28]The slow variation in DPOAE phase apparent in the data at frequencies less than roughly 3 kHz may reflect a gradual breaking of scaling symmetry in the apical turns of the cochlea. Deviations from scaling at similar frequencies are apparent in the shapes of cat auditory-nerve tuning curves (e.g., Kiang and Moxon, 1980; Liberman, 1978).

[29]Although we focus here on SFOAE phase, a few remarks about SFOAE amplitude may be helpful. In particular, we emphasize that the irregular variations in SFOAE amplitude, $|\Delta P_{\text{SFOAE}}|$, apparent in the top panel of Fig. 9 should not be confused with the quasi-periodic oscillations in ear-canal pressure amplitude, $|P_{\text{ec}}|$, seen in Figs. 1 and 2. Whereas oscillations in $|P_{\text{ec}}|$ arise due to acoustic interference between stimulus and emission caused by the quasi-periodic cycling of SFOAE phase (or, equivalently, the locally linear variation of $\angle R$) with frequency, the variations in

$|\Delta P_{\mathrm{SFOAE}}|$ result from changes in SFOAE amplitude (or, equivalently, changes in $|R|$). Frequency intervals where $|R|$ changes rapidly are known as ''anomalous regions'' (Shera and Zweig, 1993a; see also footnote 9). The theory of coherent reflection filtering accounts for the origin and properties of these irregular variations in $|R|$ with frequency (Zweig and Shera, 1995).

[30]The analysis here can be ''inverted'' by asking ''What constraint does the striking frequency independence of fixed-f_2/f_1 DPOAE phase place on cochlear mechanics?'' That constraint might reasonably be expected to take the form of a symmetry principle enforcing the empirical relation $\angle P_{\mathrm{dp}} \approx$ constant. The arguments presented here identify the underlying symmetry principle as local scaling symmetry.

[31]Bragg's law—formulated by English physicists W. H. Bragg and his son, W. L. Bragg—states that when monochromatic x rays are incident upon a crystal, diffracted beams of maximal intensity occur when the x rays that scatter back from different atomic layers within the crystal combine in phase with one another.

[32]It may be worth remarking that the principal and eponymous conclusion of this paper—namely, that mammalian OAEs arise by two fundamentally different mechanisms—while certainly consistent with the theory of coherent reflection filtering, is by no means logically dependent upon it. So far as the logic of the present paper is concerned, the existence of a plausible candidate theory for the origin of reflection-source emissions is no more than a happy coincidence.

[33]These observations are not conclusive of linearity both because the measurements have only limited precision and because *ad hoc* nonlinear systems can always be constructed that will mimic the response of a linear system to a finite collection of test signals.

[34]Just as with stimulus-frequency emissions, the forward-traveling wave scatters off perturbations in the mechanics of the cochlear partition located near the peak of the wave envelope. The backward-traveling wave reflects from the impedance mismatch at the stapes (Shera and Zweig, 1991, 1992).

[35]The extent to which these two components reflect actual distortion-source subtypes—as opposed to uncontrolled-for, level-dependent mixing of reflection- and distortion-source emissions (see Sec. IV C and Fig. 12 below)—remains an important open question.

[36]Two distortion components with differential sensitivity to acoustic trauma have also been identified in the alligator lizard (Rosowski *et al.*, 1984).

[37]To clarify the distinction we maintain between ''echo'' and ''reflection-source'' emissions: As defined in Sec. I, the term ''echo emissions'' is simply a convenient shorthand for stimulus-frequency and transiently evoked emissions; as defined by the taxonomy in Sec. IV A, the term ''reflection-source emissions'' refers to OAEs that arise by linear reflection. At low levels, echo emissions are examples of reflection-source emissions.

[38]Indeed, based on their observations Martin *et al.* (1988) suggested that SFOAEs and DPOAEs may arise by different mechanisms, a suggestion fleshed out by the taxonomy presented here.

[39]Orderly patterns of impedance perturbations typically do not contain significant components at the spatial frequencies for which scattering is coherent (Zweig and Shera, 1995).

[40]Concomitant with the small amplitudes of rabbit and rodent reflection-source emissions is the absence of pronounced DPOAE fine-structure (e.g., Whitehead *et al.*, 1992a; Whitehead, 1998). Both observations can be understood—with reference to Fig. 12—as a consequence of the relatively small amplitude of the reflection-source emission (**R**) scattered back from the f_{dp} place.

[41]At low sound-pressure levels, the width of the traveling-wave envelope can be approximated by using local scaling symmetry to convert the bandwidth of the basilar-membrane transfer function (or neural tuning curve) to a spatial distance using the cochlear map (e.g., Liberman, 1982; Greenwood, 1990). For comparison with the ratio $f_{\mathrm{dp}}/f_2 \approx 0.6$ calculated in the text, the upper-frequency $Q_{10\mathrm{dB}}$-point on the f_{dp} transfer function occurs at the frequency

$$f_{Q_{10}} \approx f_{\mathrm{dp}}(1+1/2Q_{10}).$$

For a realistic Q_{10} of order 10, this yields a frequency ratio of $f_{\mathrm{dp}}/f_{Q_{10}} \approx 0.95$, corresponding to a distance along the cochlear partition spanning less than a semitone in characteristic frequency.

[42]Of course, distortion amplitudes also depend on amplifier gains at the primary frequencies f_1 and f_2. However, because the amplifier gain saturates at high sound levels, these effects are likely to be small at the sound levels used by Martin *et al.* (i.e., 80 dB SPL).

[43]In addition, the high primary sound levels they employed may well have suppressed the gain of the f_{dp} amplifier, reducing the reflection component even in the absence of aspirin ototoxicity.

[44]To preserve the frequency scaling of the stimulus waveform, the suppressor frequency f_s should, ideally, be swept while maintaining a fixed frequency ratio f_s/f_{dp} rather than the constant frequency difference $\Delta f_s = f_s - f_{\mathrm{dp}}$ used here. However, the frequency-quantization constraints imposed by our use of digital stimulus generation and time-domain averaging precluded our use of a constant-f_s/f_{dp} paradigm. Nonetheless, control experiments suggest that the phase $\angle \Delta P_{\mathrm{dp}}$ is not especially sensitive to the precise value of f_s. Similar remarks apply to the measurement of SFOAEs discussed below.

[45]The time-domain responses Y_n and Y_{n+1} to stimulus segments X_n and X_{n+1} were judged to contain an artifact if

$$\max_i |Y_{n+1}[i] - Y_n[i]| > Y_{\mathrm{rejection}},$$

where $Y[i]$ represents the ith sample of Y, and $Y_{\mathrm{rejection}}$ is the rejection threshold (set on a per subject and per session basis). When an artifact was detected, both responses were discarded and neither Y_n nor Y_{n+1} added to the final average. We adopted this artifact-rejection scheme primarily because of the ease with which it could be implemented in real time (cf. Keefe and Ling, 1998).

Allen, J. B., and Fahey, P. F. (**1993**). ''A second cochlear-frequency map that correlates distortion product and neural tuning measurements,'' J. Acoust. Soc. Am. **94**, 809–816.

Allen, J. B., and Lonsbury-Martin, B. L. (**1993**). ''Otoacoustic emissions,'' J. Acoust. Soc. Am. **93**, 568–569.

Allen, J. B., and Neely, S. T. (**1992**). ''Micromechanical models of the cochlea,'' Phys. Today **45**, 40–47.

Brass, D., and Kemp, D. T. (**1991**). ''Time-domain observation of otoacoustic emissions during constant tone stimulation,'' J. Acoust. Soc. Am. **90**, 2415–2427.

Brass, D., and Kemp, D. T. (**1993**). ''Suppression of stimulus frequency otoacoustic emissions,'' J. Acoust. Soc. Am. **93**, 920–939.

Bredberg, G. (**1968**). ''Cellular patterns and nerve supply of the human organ of Corti,'' Acta Oto-Laryngol. Suppl. **236**, 1–135.

Brillouin, L. (**1946**). *Wave Propagation in Periodic Structures* (McGraw–Hill, New York).

Brown, A. M., and Beveridge, H. A. (**1997**). ''Two components of acoustic distortion: Differential effects of contralateral sound and aspirin,'' in *Diversity in Auditory Mechanics*, edited by E. R. Lewis, G. R. Long, R. F. Lyon, P. M. Narins, C. R. Steele, and E. L. Hecht-Poinar (World Scientific, Singapore), pp. 219–225.

Brown, A. M., and Kemp, D. T. (**1984**). ''Suppressibility of the $2f_1 - f_2$ stimulated acoustic emission in gerbil and man,'' Hearing Res. **13**, 29–37.

Brown, A. M., Harris, F. P., and Beveridge, H. A. (**1996**). ''Two sources of acoustic distortion products from the human cochlea,'' J. Acoust. Soc. Am. **100**, 3260–3267.

Brownell, W. E. (**1990**). ''Outer hair cell electromotility and otoacoustic emissions,'' Ear Hearing **11**, 82–92.

Cohen, M. F. (**1982**). ''Detection threshold microstructure and its effect on temporal integration data,'' J. Acoust. Soc. Am. **71**, 405–409.

de Boer, E. (**1980**). ''Auditory physics. Physical principles in hearing theory. I,'' Phys. Rep. **62**, 88–174.

de Boer, E. (**1983**). ''Wave reflection in passive and active cochlea models,'' in *Mechanics of Hearing*, edited by E. de Boer and M. A. Viergever (Martinus Nijhoff, The Hague), pp. 135–142.

de Boer, E. (**1984**). ''Auditory physics. Physical principles in hearing theory. II,'' Phys. Rep. **105**, 142–226.

de Boer, E. (**1991**). ''Auditory physics. Physical principles in hearing theory. III,'' Phys. Rep. **203**, 125–231.

Elliot, E. (**1958**). ''A ripple effect in the audiogram,'' Nature (London) **181**, 1076.

Engdahl, B., and Kemp, D. T. (**1996**). ''The effect of noise exposure on the details of distortion product otoacoustic emissions in humans,'' J. Acoust. Soc. Am. **99**, 1573–1587.

Engström, H., Ades, H. W., and Andersson, A. (**1966**). *Structural Pattern of the Organ of Corti* (Williams and Wilkins, Baltimore).

Fahey, P. F., and Allen, J. B. (**1997**). ''Measurement of distortion product phase in the ear canal of the cat,'' J. Acoust. Soc. Am. **102**, 2880–2891.
Gaskill, S. A., and Brown, A. M. (**1990**). ''The behavior of the acoustic distortion product, $2f_1-f_2$, from the human ear and its relation to auditory sensitivity,'' J. Acoust. Soc. Am. **88**, 821–839.
Golka, R. K. (**1994**). ''Laboratory-produced ball lightning,'' J. Geophys. Res. **99**, 10679–10681.
Greenwood, D. D. (**1990**). ''A cochlear frequency-position function for several species—29 years later,'' J. Acoust. Soc. Am. **87**, 2592–2605.
Guinan, J. J. (**1990**). ''Changes in stimulus frequency otoacoustic emissions produced by two-tone suppression and efferent stimulation in cats,'' in *Mechanics and Biophysics of Hearing*, edited by P. Dallos, C. D. Geisler, J. W. Matthews, M. A. Ruggero, and C. R. Steele (Springer-Verlag, New York), pp. 170–177.
Gummer, A. W., Smolders, J. W. T., and Klinke, R. (**1987**). ''Basilar membrane motion in the pigeon measured with the Mössbauer technique,'' Hearing Res. **29**, 63–92.
Hartmann, W. M. (**1997**). *Signal, Sound, and Sensation* (AIP, Woodbury, NY).
Heitmann, J., Waldman, B., Schnitzler, H. U., Plinkert, P. K., and Zenner, H.-P. (**1997**). ''Suppression growth functions of DPOAE with a suppressor near $2f_1-f_2$ depends on DP fine structure: Evidence for two generation sites for DPOAE,'' Assoc. Res. Otolaryngol. Abs. **20**, 83.
Heitmann, J., Waldman, B., Schnitzler, H. U., Plinkert, P. K., and Zenner, H.-P. (**1998**). ''Suppression of distortion product otoacoustic emissions (DPOAE) near $2f_1-f_2$ removes DP-gram fine structure—Evidence for a secondary generator,'' J. Acoust. Soc. Am. **103**, 1527–1531.
Kanis, L. J., and de Boer, E. (**1997**). ''Frequency dependence of acoustic distortion products in a locally active model of the cochlea,'' J. Acoust. Soc. Am. **101**, 1527–1531.
Keefe, D. H., and Ling, R. (**1998**). ''Double-evoked otoacoustic emissions. II. Intermittent noise rejection, calibration and ear-canal measurements,'' J. Acoust. Soc. Am. **103**, 3499–3508.
Kemp, D. T. (**1978**). ''Stimulated acoustic emissions from within the human auditory system,'' J. Acoust. Soc. Am. **64**, 1386–1391.
Kemp, D. T. (**1979a**). ''Evidence of mechanical nonlinearity and frequency selective wave amplification in the cochlea,'' Arch. Otorhinolaryngol. **224**, 37–45.
Kemp, D. T. (**1979b**). ''The evoked cochlear mechanical response and the auditory microstructure—Evidence for a new element in cochlear mechanics,'' Scand. Audiol. Suppl. **9**, 35–47.
Kemp, D. T. (**1980**). ''Towards a model for the origin of cochlear echoes,'' Hearing Res. **2**, 533–548.
Kemp, D. T. (**1986**). ''Otoacoustic emissions, travelling waves and cochlear mechanisms,'' Hearing Res. **22**, 95–104.
Kemp, D. T. (**1997**). ''Otoacoustic emissions in perspective,'' in *Otoacoustic Emissions: Clinical Applications*, edited by M. S. Robinette and T. J. Glattke (Thieme, New York), pp. 1–21.
Kemp, D. T. (**1998**). ''Otoacoustic emissions: Distorted echoes of the cochlea's travelling wave,'' in *Otoacoustic Emissions: Basic Science and Clinical Applications*, edited by C. I. Berlin (Singular, San Diego), pp. 1–59.
Kemp, D. T., and Brown, A. M. (**1983a**). ''A comparison of mechanical nonlinearities in the cochleae of man and gerbil from ear canal measurements,'' in *Hearing—Physiological Bases and Psychophysics*, edited by R. Klinke and R. Hartmann (Springer-Verlag, Berlin), pp. 75–82.
Kemp, D. T., and Brown, A. M. (**1983b**). ''An integrated view of cochlear mechanical nonlinearities observable from the ear canal,'' in *Mechanics of Hearing*, edited by E. de Boer and M. A. Viergever (Martinus Nijhoff, The Hague), pp. 75–82.
Kemp, D. T., and Chum, R. A. (**1980**). ''Observations on the generator mechanism of stimulus frequency acoustic emissions—Two tone suppression,'' in *Psychophysical Physiological and Behavioural Studies in Hearing*, edited by G. V. D. Brink and F. A. Bilsen (Delft U.P., Delft), pp. 34–42.
Kemp, D. T., and Knight, R. (**1999**). ''Virtual DP reflector explains DPOAE 'wave' and 'place' fixed dichotomy,'' Assoc. Res. Otolaryngol. Abs. **22**, 396.
Kemp, D. T., Bray, P., Alexander, L., and Brown, A. M. (**1986**). ''Acoustic emission cochleography—Practical aspects,'' Scand. Audiol. Suppl. **25**, 71–95.
Kemp, D. T., Brass, D., and Souter, M. (**1990**). ''Observations on simultaneous SFOAE and DPOAE generation and suppression,'' in *Mechanics and Biophysics of Hearing*, edited by P. Dallos, C. D. Geisler, J. W. Matthews, M. A. Ruggero, and C. R. Steele (Springer-Verlag, New York), pp. 202–209.
Kiang, N. Y. S., and Moxon, E. C. (**1980**). ''Tails of tuning curves of auditory-nerve fibers,'' J. Acoust. Soc. Am. **68**, 1115–1122.
Kim, D. O. (**1980**). ''Cochlear mechanics: Implications of electrophysiological and acoustical observations,'' Hearing Res. **2**, 297–317.
Kimberley, B. P., Brown, D. K., and Eggermont, J. J. (**1993**). ''Measuring human cochlear traveling wave delay using distortion product emission phase responses,'' J. Acoust. Soc. Am. **94**, 1343–1350.
Kössl, M., and Vater, M. (**1995**). ''Cochlear structure and function in bats,'' in *Hearing by Bats*, edited by A. N. Popper and R. R. Fay (Springer-Verlag, New York), pp. 191–234.
Kummer, P., Janssen, T., and Arnold, W. (**1995**). ''Suppression tuning characteristics of the $2f_1-f_2$ distortion-product otoacoustic emission in humans,'' J. Acoust. Soc. Am. **98**, 197–210.
Leff, H. S., and Rex, A. F., editors (**1990**). *Maxwell's Demon: Entropy, Information, Computing* (Princeton U.P., Princeton).
Liberman, M. C. (**1978**). ''Auditory-nerve response from cats raised in a low-noise chamber,'' J. Acoust. Soc. Am. **63**, 442–455.
Liberman, M. C. (**1982**). ''The cochlear frequency map for the cat: Labeling auditory-nerve fibers of known characteristic frequency,'' J. Acoust. Soc. Am. **72**, 1441–1449.
Long, G. R. (**1984**). ''The microstructure of quiet and masked thresholds,'' Hearing Res. **15**, 73–87.
Lonsbury-Martin, B. L., Martin, G. K., Probst, R., and Coats, A. C. (**1988**). ''Spontaneous otoacoustic emissions in the nonhuman primate. II. Cochlear anatomy,'' Hearing Res. **33**, 69–94.
Martin, G. K., Lonsbury-Martin, B. L., Probst, R., and Coats, A. C. (**1988**). ''Spontaneous otoacoustic emissions in the nonhuman primate. I. Basic features and relations to other emissions,'' Hearing Res. **33**, 49–68.
Maxwell, J. C. (**1871**). *Theory of Heat* (Longmans, Green, London).
Mills, D. M., and Rubel, E. W. (**1994**). ''Variation of distortion product otoacoustic emissions with furosemide injection,'' Hearing Res. **77**, 183–199.
Nakajima, H. H., Olson, E. S., Mountain, D. C., and Hubbard, A. E. (**1994**). ''Electrically evoked otoacoustic emissions from the apical turns of the gerbil cochlea,'' J. Acoust. Soc. Am. **96**, 786–794.
Nakajima, H. H., Naidu, R. C., Hubbard, A. E., and Mountain, D. C. (**1999**). ''Forward and reverse traveling waves in the cochlea,'' Assoc. Res. Otolaryngol. Abs. **22**, 333.
Neely, S. T., and Stover, L. J. (**1997**). ''A generation of distortion products in a model of cochlear mechanics,'' in *Diversity in Auditory Mechanics*, edited by E. R. Lewis, G. R. Long, R. F. Lyon, P. M. Narins, C. R. Steele, and E. L. Hecht-Poinar (World Scientific, Singapore), pp. 434–440.
Norton, S. J., and Neely, S. T. (**1987**). ''Tone-burst-evoked otoacoustic emissions from normal-hearing subjects,'' J. Acoust. Soc. Am. **81**, 1860–1872.
Norton, S. J., and Rubel, E. W. (**1990**). ''Active and passive ADP components in mammalian and avian ears,'' in *Mechanics and Biophysics of Hearing*, edited by P. Dallos, C. D. Geisler, J. W. Matthews, M. A. Ruggero, and C. R. Steele (Springer-Verlag, Berlin), pp. 219–226.
Norton, S. J., and Stover, L. J. (**1994**). ''Otoacoustic emissions: An emerging clinical tool,'' in *Handbook of Clinical Audiology*, edited by J. Katz (Williams and Wilkins, Baltimore), pp. 448–462.
O'Mahoney, C. F., and Kemp, D. T. (**1995**). ''Distortion product otoacoustic emission delay measurement in human ears,'' J. Acoust. Soc. Am. **97**, 3721–3735.
Patuzzi, R. (**1996**). ''Cochlear micromechanics and macromechanics,'' in *The Cochlea*, edited by P. Dallos, A. N. Popper, and R. R. Fay (Springer-Verlag, New York), pp. 186–257.
Probst, R., Lonsbury-Martin, B. L., and Martin, G. K. (**1991**). ''A review of otoacoustic emissions,'' J. Acoust. Soc. Am. **89**, 2027–2067.
Puria, S., and Rosowski, J. J. (**1997**). ''Measurement of reverse transmission in the human middle ear: Preliminary results,'' in *Diversity in Auditory Mechanics*, edited by E. R. Lewis, G. R. Long, R. F. Lyon, P. M. Narins, C. R. Steele, and E. L. Hecht-Poinar (World Scientific, Singapore), pp. 151–157.
Puria, S., Peake, W. T., and Rosowski, J. J. (**1997**). ''Sound-pressure measurements in the cochlear vestibule of human-cadaver ears,'' J. Acoust. Soc. Am. **101**, 2754–2770.
Rhode, W. S. (**1971**). ''Observations of the vibration of the basilar membrane in squirrel monkeys using the Mössbauer technique,'' J. Acoust. Soc. Am. **49**, 1218–1231.
Rhode, W. S., and Cooper, N. P. (**1996**). ''Nonlinear mechanics in the apical

turn of the chinchilla cochlea *in vivo*,'' Aud. Neurosci. **3**, 101–121.
Robinette, M. S., and Glattke, T. J., editors (**1997**). *Otoacoustic Emissions: Clinical Applications* (Thieme, New York).
Rosowski, J. J., Peake, W. T., and White, J. R. (**1984**). ''Cochlear nonlinearities inferred from two-tone distortion products in the ear canal of the alligator lizard,'' Hearing Res. **13**, 141–158.
Shera, C. A. (**1992**). ''Listening to the Ear,'' Ph.D. thesis, California Institute of Technology.
Shera, C. A., and Guinan, J. J. (**1997**). ''Measuring cochlear amplification and nonlinearity using distortion-product otoacoustic emissions as a calibrated intracochlear sound source,'' Assoc. Res. Otolaryngol. Abs. **20**, 51.
Shera, C. A., and Guinan, J. J. (**1998**). ''Reflection emissions and distortion products arise by fundamentally different mechanisms,'' Assoc. Res. Otolaryngol. Abs. **21**, 344.
Shera, C. A., and Zweig, G. (**1991**). ''Reflection of retrograde waves within the cochlea and at the stapes,'' J. Acoust. Soc. Am. **89**, 1290–1305.
Shera, C. A., and Zweig, G. (**1992**). ''Analyzing reverse middle-ear transmission: Noninvasive Gedankenexperiments,'' J. Acoust. Soc. Am. **92**, 1371–1381.
Shera, C. A., and Zweig, G. (**1993a**). ''Noninvasive measurement of the cochlear traveling-wave ratio,'' J. Acoust. Soc. Am. **93**, 3333–3352.
Shera, C. A., and Zweig, G. (**1993b**). ''Order from chaos: Resolving the paradox of periodicity in evoked otoacoustic emission,'' in *Biophysics of Hair Cell Sensory Systems*, edited by H. Duifhuis, J. W. Horst, P. van Dijk, and S. M. van Netten (World Scientific, Singapore), pp. 54–63.
Siebert, W. M. (**1968**). ''Stimulus transformations in the peripheral auditory system,'' in *Recognizing Patterns*, edited by P. A. Kolers and M. Eden (MIT, Cambridge), pp. 104–133.
Siegel, J. H., Dreisbach, L. E., Neely, S. T., and Spear, W. H. (**1998**). ''Vector decomposition of distortion-product otoacoustic emission sources in humans,'' Assoc. Res. Otolaryngol. Abs. **21**, 347.
Sondhi, M. M. (**1978**). ''Method for computing motion in a two-dimensional cochlear model,'' J. Acoust. Soc. Am. **63**, 1468–1477.
Souter, M. (**1995**). ''Stimulus frequency otoacoustic emissions from guinea pig and human subjects,'' Hearing Res. **90**, 1–11.
Strube, H. W. (**1989**). ''Evoked otoacoustic emissions as cochlear Bragg reflections,'' Hearing Res. **38**, 35–45.
Talmadge, C. L., and Tubis, A. (**1993**). ''On modeling the connection between spontaneous and evoked otoacoustic emissions,'' in *Biophysics of Hair Cell Sensory Systems*, edited by H. Duifhuis, J. W. Horst, P. van Dijk, and S. M. van Netten (World Scientific, Singapore), pp. 25–32.
Talmadge, C. L., Tubis, A., Piskorski, P., and Long, G. (**1997**). ''Modeling otoacoustic emission fine structure,'' in *Diversity in Auditory Mechanics*, edited by E. R. Lewis, G. R. Long, R. F. Lyon, P. M. Narins, C. R. Steele, and E. L. Hecht-Poinar (World Scientific, Singapore), pp. 462–471.
Talmadge, C. L., Tubis, A., Long, G. R., and Piskorski, P. (**1998a**). ''Modeling otoacoustic emission and hearing threshold fine structures,'' J. Acoust. Soc. Am. **104**, 1517–1543.
Talmadge, C. L., Long, G. R., Tubis, A., and Dhar, S. (**1998b**). ''Study of cochlear reflectance using distortion product otoacoustic emissions,'' Assoc. Res. Otolaryngol. Abs. **21**, 345.
Talmadge, C. L., Long, G. R., Tubis, A., and Dhar, S. (**1999**). ''Experimental confirmation of the two-source interference model for the fine structure of distortion product otoacoustic emissions,'' J. Acoust. Soc. Am. **105**, 275–292.
Thomas, I. B. (**1975**). ''Microstructure of the pure-tone threshold,'' J. Acoust. Soc. Am. Suppl. 1 **57**, S26–S27.
van Hengel, P. W. J. (**1996**). ''Emissions from cochlear modelling,'' Ph.D. thesis, Rijksuniversiteit Groningen.
Ver, I. L., Brown, R. M., and Kiang, N. Y. S. (**1975**). ''Low-noise chambers for auditory research,'' J. Acoust. Soc. Am. **58**, 392–398.
Whitehead, M. L. (**1998**). ''Species differences of distortion-product otoacoustic emissions: Comment on ''Interpretation of distortion product otoacoustic emission measurements. I. Two stimulus tones'' [J. Acoust. Soc. Am. **102**, 413–429 (1997)],'' J. Acoust. Soc. Am. **103**, 2740–2742.
Whitehead, M. L., Lonsbury-Martin, B. L., and Martin, G. K. (**1992a**). ''Evidence for two discrete sources of $2f_1-f_2$ distortion-product otoacoustic emission in rabbit: I. Differential dependence on stimulus parameters,'' J. Acoust. Soc. Am. **91**, 1587–1607.
Whitehead, M. L., Lonsbury-Martin, B. L., and Martin, G. K. (**1992b**). ''Evidence for two discrete sources of $2f_1-f_2$ distortion-product otoacoustic emission in rabbit: II. Differential physiological vulnerability,'' J. Acoust. Soc. Am. **92**, 2662–2682.
Whitehead, M. L., Lonsbury-Martin, B. L., Martin, G. K., and McCoy, M. J. (**1996a**). ''Otoacoustic emissions: Animal models and clincal observations,'' in *Clinical Aspects of Hearing*, edited by T. R. V. D. Water, A. N. Popper, and R. R. Fay (Springer-Verlag, New York), pp. 199–257.
Whitehead, M. L., Stagner, B. B., Martin, G. K., and Lonsbury-Martin, B. L. (**1996b**). ''Visualization of the onset of distortion-product otoacoustic emissions and measurement of their latency,'' J. Acoust. Soc. Am. **100**, 1663–1679.
Whitehead, M. L., Stagner, B. B., McCoy, M. J., Lonsbury-Martin, B. L., and Martin, G. K. (**1995**). ''Dependence of distortion-product otoacoustic emissions on primary levels in normal and impaired ears. II. Asymmetry in L_1, L_2 space,'' J. Acoust. Soc. Am. **97**, 2359–2377.
Wier, C. C., Pasanen, E. G., and McFadden, D. (**1988**). ''Partial dissociation of spontaneous otoacoustic emissions and distortion products during aspirin use in humans,'' J. Acoust. Soc. Am. **84**, 230–237.
Wilson, J. P. (**1980**). ''Evidence for a cochlear origin for acoustic re-emissions, threshold fine-structure and tonal tinnitus,'' Hearing Res. **2**, 233–252.
Wit, H. P., and Ritsma, R. J. (**1979**). ''Stimulated acoustic emissions from the human ear,'' J. Acoust. Soc. Am. **66**, 911–913.
Withnell, R. H., and Yates, G. K. (**1998**). ''Enhancement of the transient-evoked otoacoustic emission produced by the addition of a pure tone in the guinea pig,'' J. Acoust. Soc. Am. **104**, 344–349.
Wright, A. A. (**1984**). ''Dimensions of the cochlear stereocilia in man and in guinea pig,'' Hearing Res. **13**, 89–98.
Yates, G. K., and Withnell, R. H. (**1998**). ''Intermodulation distortion in click-evoked otoacoustic emissions,'' Assoc. Res. Otolaryngol. Abs. **21**, 17.
Zurek, P. M. (**1985**). ''Acoustic emissions from the ear: A summary of results from humans and animals,'' J. Acoust. Soc. Am. **78**, 340–344.
Zweig, G. (**1976**). ''Basilar membrane motion,'' in *Cold Spring Harbor Symposia on Quantitative Biology, Volume XL, 1975* (Cold Spring Harbor Laboratory, Cold Spring Harbor, NY), pp. 619–633.
Zweig, G., and Shera, C. A. (**1995**). ''The origin of periodicity in the spectrum of evoked otoacoustic emissions,'' J. Acoust. Soc. Am. **98**, 2018–2047.
Zwicker, E. (**1983**). ''Delayed evoked oto-acoustic emissions and their suppression by gaussian-shaped pressure impulses,'' Hearing Res. **11**, 359–371.
Zwicker, E., and Schloth, E. (**1984**). ''Interrelation of different oto-acoustic emissions,'' J. Acoust. Soc. Am. **75**, 1148–1154.